

CHAPTER 23

HV Direct-Current Transmission

Originally electrical power generation, transmission, and distribution systems were direct current. The advent of the three-phase induction motor and the ability of transformers to convert one ac voltage to another ac voltage level (at the same frequency), saw the unassailable rise to dominance of ac electrical power systems. But for long distance electrical power overhead line transmission, of just a few hundred kilometres of typically about 300 to 550km, a dc transmission system is a viable possibility. For underwater or underground electrical power transmission, ac may not be viable at just 50km due to high capacitive charging currents because of the close proximity of the cables (particularly subsea cables). Typical application boundaries between the use of HVAC and HVDC are shown in figure 23.1. The 1980km HVDC link between Xiangjiaba and Shanghai is the largest dc overhead line in the world, with a capacity of 6.4GW and a ± 800 kV DC link voltage. The longest overhead HVDC of 2,375 km (3.15GW ± 600 kV) is the Rio Madeira link in Brazil. A Brazilian functional HVDC transmission system is rated at ± 600 kV on 785km and 805km transmission lines. Each of the two bipolar dc transmission systems carry 3.15GW. Also involved are three, three-phase 765kV ac lines which are 1GVAr variable capacitor series compensated (FACTS) at two intermediate substations.

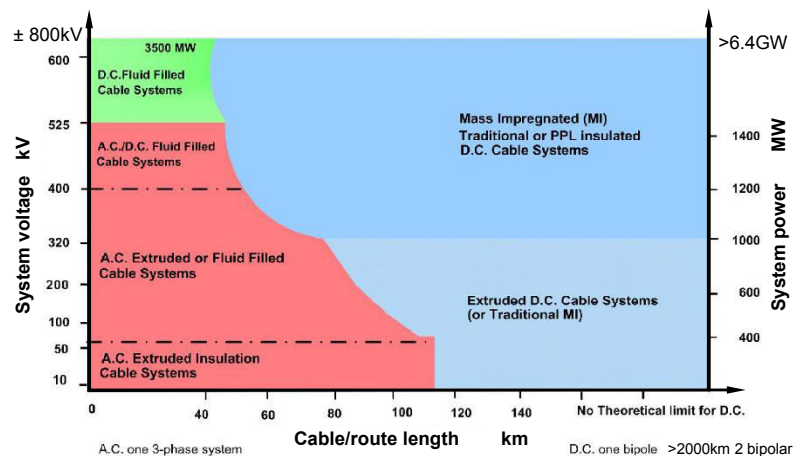


Figure 23.1. HVDC and HVAC transmission system operational boundaries.

23.1 HVDC electrical power transmission

Electrical power is generated in ac form and is also usually distributed and consumed in an ac form. Its long distance transmission between these two stages may be an ac or a dc transmission system. In a high-voltage dc (HVDC) system the generated 50/60Hz ac is controlled-rectified to dc, transmitted, then at the receiving end, converted from dc back to 50/60Hz ac. A HVDC system is two ac systems connected by a dc transmission system, where the ac systems can be totally independent.

The dc-link of a HVDC transmission system is either

- a controlled voltage dc-link or
- a controlled current dc-link.

A HVDC controlled *current link* has the following characteristics.

The link is highly inductive, achieved with series inductance at each end.

The converter/inverter technology is operated in a controlled current mode, thus the converter/inverter devices require reverse voltage blocking ability. Symmetrical blocking thyristor devices are applicable, but such devices are restricted to line commutation and phased control.

A HVDC controlled *voltage link* has the following characteristics.

The link is highly capacitive, achieved with parallel connected capacitance at each end.

The converter/inverter technology is operated in a controlled voltage mode, thus the converter/inverter devices can be uni-directional voltage blocking IGBT technology. Since devices are gate commutable, a switching frequency of kHz's is possible, thus PWM techniques can be employed for harmonic minimisation.

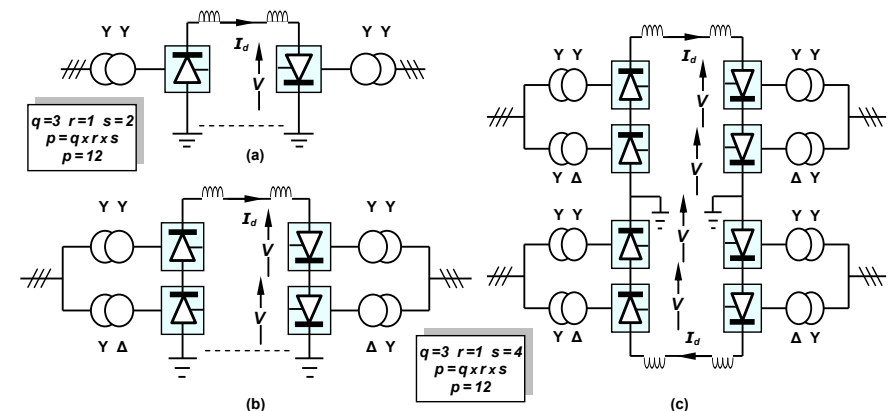


Figure 23.2. HVDC transmission systems: (a) 6 pulse monopole; (b) 12 pulse monopole; and (c) 12 pulse bipolar, converter bridge configurations.

23.2 HVDC configurations (also see section 23.16)

There are a number of different configurations for transmitting dc power, depending on the number of cables employed. Each uses a three-phase fully-controlled thyristor converter (rectifier) coupled through a dc link to another identical three-phase fully-controlled thyristor converter (inverter). Both converters have the same modular structure except the converter connections to the dc link are interchanged for one converter, hence power flow is fully reversible. Since the valves can only conduct current in one direction, power reversal is achieved by changing the polarity of the dc link terminal voltages through control of the converter thyristor firing delay angles. The rectification mode (positive dc link voltage) is achieved with thyristor firing angles of $0 < \alpha < \frac{1}{2}\pi$ while inversion (negative dc link voltage) is achieved with firing angles of $\frac{1}{2}\pi < \alpha < \pi$. Because one converter terminal connection is reversed, a rectifying voltage ($0 < \alpha < \frac{1}{2}\pi$) is opposed by an inverting voltage ($\frac{1}{2}\pi < \alpha < \pi$) – subtractive not additive voltages.

23.2i - Monopole and earth return

The monopole configurations shown in figure 23.2 parts a and b (6 pulse and 12 pulse respectively) use just one transmission cable and earth (where resistance is dominated by the earth electrodes each end) is used as the negative return. Occasionally, a metal earth return may be used, but importantly any return is at ground potential thus does not need the full transmission voltage insulation. The converter output terminals are reversed relative to one another, as indicated by the direction of the thyristors in the symbol blocks.

Issues involved in using a ground return are

- Electrochemical corrosion of buried metals objects, like pipelines
- Electrode chemical reaction under the sea
- Magnetic field disturbances when the go and return paths become unbalanced

The monopole system is limited in power handling capability, typically 1.5GW above the ground, and 600MW below the ground or under the sea.

23.2ii - Bipolar

In the bipolar arrangement two high voltage conductors, at opposite potentials with respect to ground, are used as shown in figure 23.2c and figure 23.3 in more detail. Any pole imbalance uses an earth return, if a low-voltage metal ground return is not used. The bipolar configuration has a number of advantages over the monopole arrangement.

- Normally no earth-current flows which minimises earth losses and any earth related environmental effects, including minimal corrosion of underground system metal components
- If a fault develops on one pole, the other pole can continue to operate in a monopole arrangement, using the earth as the return path
- For a given power rating, each conductor has half the cross-sectional area of the monopole line, thus reducing the extra cost of using a second conductor
- The same dc transmission line towers can carry two lines with a small additional capital cost

A homopolar hvdc link is formed if the two high voltage conductors have the same polarity, with, undesirably, a high ground or metal return current.

The bipolar system is capable of higher transmission powers than the monopole configuration. Bipolar systems can carry over 3GW at voltages of over ±500kV, over distances well in excess of 1000km.

23.2iii - Tripole

Two of the three conductors of an ac system are used in a bipolar configuration, with the third conductor used as a parallel monopole with bidirectional power flow capability. The bidirectional capability of the third conductor allows each of the two bipolar conductors to carry higher than rated current when each in turn is relieved periodically by the monopole system, such that all three conductors do not exceed rated I^2R losses. In this way each of the three conductors experience the same thermal losses. This is achieved if the bipolar currents are cycled every few minutes between $0.366pu \cdot \frac{1}{2}(\sqrt{3}-1)$ and $1.366 pu \cdot \frac{1}{2}(\sqrt{3}+1)$, with ±1 pu being appropriately alternated in the monopole. As a result, 80% more power can be transmitted compared with the ac equivalent, using the same conductors, towers, etc. Unlike the ac equivalent, the dc system can be fully loaded without system instability or need for reactive power compensation.

23.2iv - Back-to-back

Two different asynchronous ac systems in close proximity, possibly operating at different frequencies, can be interconnected by either a monopole or bipolar system. Since no dc transmission cables are necessary, because of the close proximity of the two systems, the system type and voltage level are not restrictive.

23.2v - Multi-terminal

More than two converters are connected to the same dc link, where simultaneously, at least one converter operates in the rectification mode and at least one other converter operates in an inversion mode. Mechanical switching of the converter terminals is necessary. The control system is more elaborate than for normal point-to-point transmission and power reversal is affected by current reversal, (as opposed to the usual voltage reversal used in point-to-point transmission). See section 23.12.

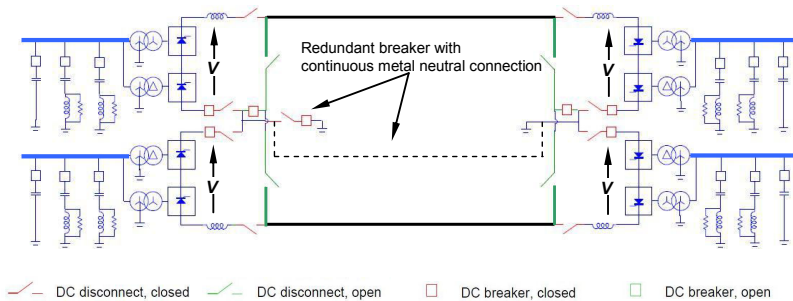


Figure 23.3: Bipolar HVDC system with station optional metallic return.

Current Source converter HVDC transmission systems

The thyristor current source converter approach is well established and its reliability has been proven. Most existing dc transmission systems are based on current source converter technology. HVDC transmission systems based on current source technology can use line-commutated converters LCC or capacitor commutated converters CCC. Fig. 23.4 shows the line and capacitor commutated converter HVDC transmission systems. In the CCC converter case, the series commutation capacitors can be on either side of the line voltage transformers and generate reactive power proportional to the load current. When series capacitors are used on the line side, before the ac filters, the configuration may include parallel reactors and TCSC thyristor valves, forming a Controlled Series Capacitor Converter, CSCC.

The capacitor commutated converter extends the applications of the HVDC transmission systems based on current source converters to systems with a low short circuit ratio. This converter improves system immunity to the risk of commutation failure; replaces the switch capacitors by a combination of fixed capacitors and reactors for filtering purposes only, and reduces transformer rating and size. As a result, the size of the converter station in CCC-HVDC transmission systems is reduced compare to a LCC-HVDC system with the same power rating. The capacitor-commutating converter can be connected to ac systems with a short circuit ratio as low as 1.0 without the need for a synchronous condenser or static synchronous compensator (STATCOM) to provide additional reactive power and can maintain constant voltage at the point of common coupling.

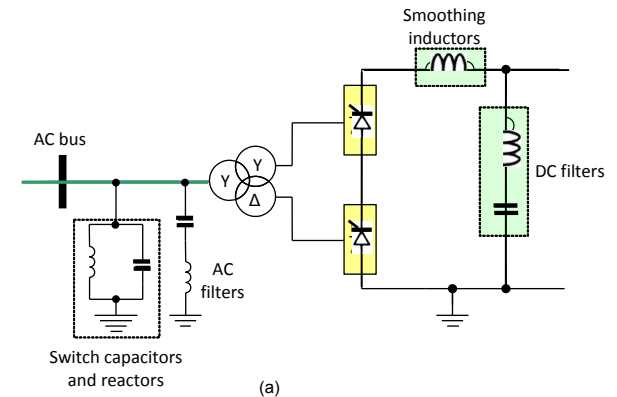
According to IEEE Standard 1204-1997, the system short circuit ratio (SCR) and effective short circuit ratio (ESCR) are defined as:

$$SCR = \frac{S}{P_{dc}}$$

$$ESCR = \frac{S - Q_c}{P_{dc}}$$

where S is the ac system three-phase symmetrical short circuit level in MVA at the converter terminal (ac bus) calculated at rated terminal voltage (1 pu), P_{dc} is the rated dc power of the terminal in MW, and Q_c is the three-phase fundamental MVar at rated P_{dc} and rated terminal voltage. This includes ac filters and shunt connected reactive power capacitors used to compensate for the reactive power absorbed by the converter. The system strength is classified as follows:

- system is strong if $SCR > 3$ or $ESCR > 2.5$
- system is weak if $3 > SCR > 2$ or $2.5 > ESCR > 1.5$
- system is very weak (very low SCR) if $SCR < 2$ or $ESCR < 1.5$



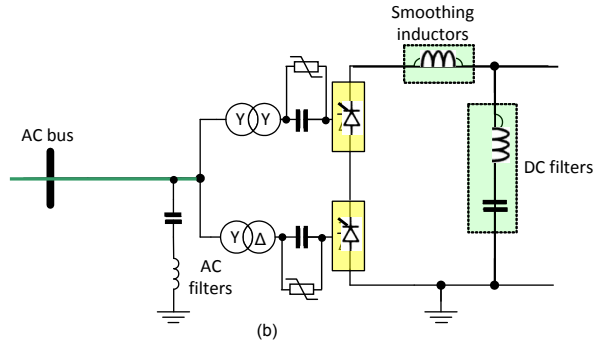


Figure 23.4: Converter station technologies for the current source based HVDC transmission systems: (a) line commutated high voltage dc (LCC-HVDC) transmission system and (b) series capacitor (valve side) commutated high voltage dc (CCC-HVDC) transmission system.

23.3 Typical thyristor HVDC transmission system

A fully modular hardware structure is used. The few watts needed for gate power is harvested from thyristor anode level components.

Each 8.8kV symmetrically blocking thyristor is configured in a module with its gate electronics and RC snubber as shown in figure 23.5. Many thyristors are connected in series to form a valve, with internal static voltage sharing resistors and a saturable reactor turn-on snubber as shown in figure 23.5a. The saturable reactor usually incorporates shunt damping to control turn-on current oscillation at saturation.

Six valves are needed to form the 6 pulse valve group converter bridge in figure 23.6a, while 12 valves are used to form the twelve pulse value group converter in figure 23.6b. Each group of four valves in a single vertical stack form quadrivalves as shown in figure 23.6b. Each quadrivalve may contain hundreds of series connected thyristors to give the necessary hundreds of kV pole voltage rating.

Typical six and twelve pulse valve group configurations are shown in figure 23.6, which form the unipolar converters in figure 23.2 parts a and b respectively. A more detailed circuit diagram of the 12-pulse converter and its MOV voltage protection and dc and ac harmonic filtering circuitry, in a substation installation, is shown in figure 23.7. The dc inductors L_{dc} in each pole assist in filtering harmonic currents and smooth the dc side current thereby reducing the current level for the onset of discontinuous current flow. Because the inductors control the dc link side di/dt , converter commutation is more robust. No dc filters may be necessary with the back-to-back HVDC converter configuration.

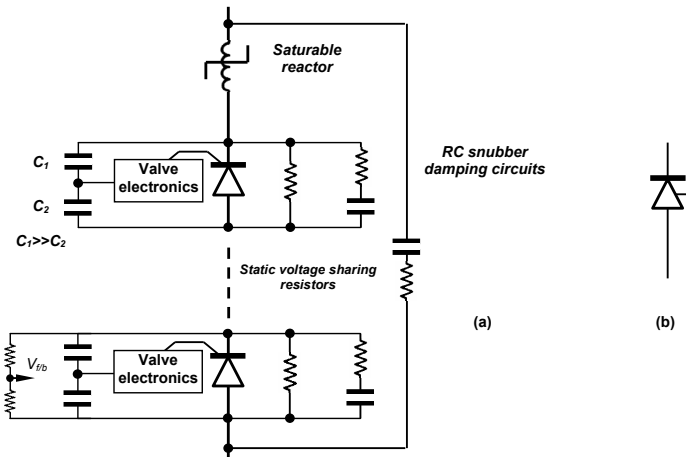


Figure 23.5: Thyristor valve: (a) modules components assembled into a valve and (b) valve symbol.

23.4 Twelve-pulse ac line frequency converters

The six-pulse line-frequency fully-controlled thyristor converter was discussed in chapter 14.6. Harmonic filters are required on both the ac and dc side of the converter as shown in figure 23.7. The ac side harmonics occur at $6n \pm 1$ the fundamental, while the dc side harmonics are generated at $6n$. To reduce the filtering requirements, and increase the effectiveness of the filtering, on both the ac and dc sides, most high power HVDC systems use 12-pulse, 30° phase-shifted transformer/converter arrangements. The ac side harmonics now occur at $12n \pm 1$ and the dc components are generated at $12n$. Twelve-pulse converter operation is achieved by using the series bridge connection in conjunction with Δ -Y and Y-Y compound connected transformers as shown in figure 23.6b. (A delta connection is usually employed on the lower voltage side of the transformer.) Figure 23.11a shows the arrangement in more detail, with the necessary transformer turns ratio to ensure each converter bridge produces the same output voltage at the same thyristor firing delay angle. Voltage matching between the ac line and required dc link voltage is achieved with the transformer turns ratio N , shown in figure 23.11a. The series thyristors in each bridge provide paths which allow both converter currents to be equal.

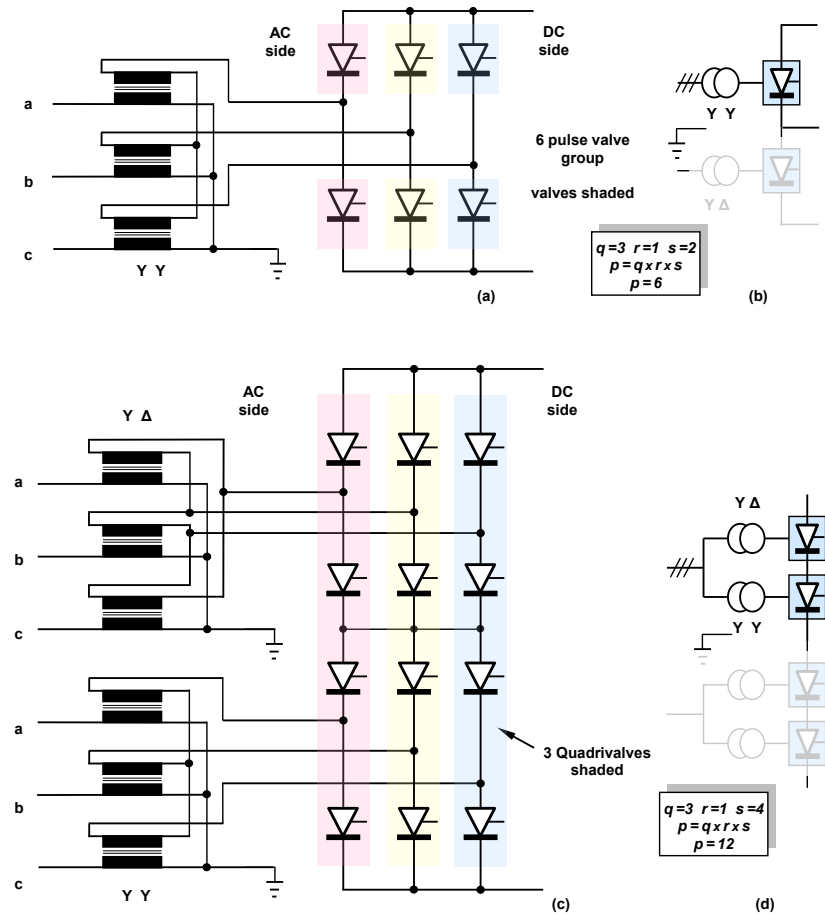


Figure 23.6. Monopole converter bridges: Six-pulse valve group (a) converter bridge schematic and (b) six-pulse valve group converter symbol; Twelve-pulse star valve group connected configuration with star-star and star-delta connected converter transformers: (c) converter schematic and (d) twelve-pulse valve group converter symbol.

As a result of the transformer configuration, the corresponding upper and lower transformer voltages are displaced by 30° , where V_{aYs-nY} leads $V_{a\Delta s-n\Delta}$ by $\frac{1}{6}\pi$ radians. The dc-link current I_d is assumed constant because of the large smoothing inductor L_{dc} (linear and typically $\frac{1}{2}$ H). If source impedance is neglected, then the various circuit current waveforms are constituted from rectangular current blocks as shown in figure 23.11b. Each converter operates with the same firing delay angle α , with respect to the voltage references shown in figure 23.11b. Because the transformer primaries are in parallel, the input current is the sum of the appropriate two transformer phase currents, namely $i_a = i_{Ys} + i_{\Delta s}$ for phase a. The Fourier series for each transformer primary phase current is obtained from analysis of the appropriate six-pulse converter current, for each converter

$$i_{Ys} = \frac{2\sqrt{3} I_d}{N\pi} \left(\cos \theta - \frac{1}{5} \cos 5\theta + \frac{1}{7} \cos 7\theta - \frac{1}{11} \cos 11\theta + \frac{1}{13} \cos 13\theta \dots \right) \quad (23.1)$$

and

$$i_{\Delta s} = \frac{2\sqrt{3} I_d}{N\pi} \left(\cos \theta + \frac{1}{5} \cos 5\theta - \frac{1}{7} \cos 7\theta - \frac{1}{11} \cos 11\theta + \frac{1}{13} \cos 13\theta \dots \right) \quad (23.2)$$

Because of the symmetry of a three-phase system, no triplens exist in each input current. The total line current drawn is

$$i_a = i_{Ys} + i_{\Delta s} = \frac{4\sqrt{3} I_d}{N\pi} \left(\cos \theta - \frac{1}{11} \cos 11\theta + \frac{1}{13} \cos 13\theta - \frac{1}{23} \cos 23\theta \dots \right) \quad (23.3)$$

The 12-pulse transformer/converter arrangement cancels harmonic components $6 \times (2n-1) \pm 1$.

The line current i_a rms value is $(1 + \frac{1}{\sqrt{3}}) I_d / N$ and the rms fundamental is $2\sqrt{6} I_d / N\pi$.

The ac line current harmonics occur at $12n \pm 1$. The valve side ac line current, shown as $N \times I_{Ys}$ (or $N \times I_{\Delta s}$) in figure 23.11b has an rms value of $I_d \sqrt{2/3}$, and once rectified, the valve unipolar current has an rms value of $I_d / \sqrt{3}$.

More general equations are for the general case of asymmetrical converter firing when $\alpha_1 \neq \alpha_2$. Assuming a turns ratio between the phase windings of the star connected primary and the star connected secondary is 2:1, and the turns ratio between the primary and the delta connected secondary is $2:\sqrt{3}$, then

$$i_a = \frac{1}{2} i_{Ys} + \frac{\sqrt{3}}{2} i_{\Delta s} \quad (23.4)$$

Due to waveform symmetry, no dc component or even harmonics exist.

The Fourier coefficients a_{nY} and b_{nY} of i_{Ys} ($= a_{nY} + j b_{nY}$) are

$$a_{nY} = \frac{1}{\pi} \int_0^{2\pi} i_{Ys}(t) \cos n\omega t \, d\omega t = \frac{1}{\pi} \left[\int_{\frac{5\pi}{6} + \alpha_1}^{\frac{11\pi}{6} + \alpha_1} I_d \cos n\omega t \, d\omega t - \int_{\frac{7\pi}{6} + \alpha_1}^{\frac{\pi}{6} + \alpha_1} I_d \cos n\omega t \, d\omega t \right] \quad (23.5)$$

$$= -\frac{4I_d}{n\pi} \sin \frac{n\pi}{3} \sin n\alpha_1 \quad n = 1, 3, 5, \dots$$

$$b_{nY} = \frac{1}{\pi} \int_0^{2\pi} i_{Ys}(t) \sin n\omega t \, d\omega t = \frac{1}{\pi} \left[\int_{\frac{5\pi}{6} + \alpha_1}^{\frac{11\pi}{6} + \alpha_1} I_d \sin n\omega t \, d\omega t - \int_{\frac{7\pi}{6} + \alpha_1}^{\frac{\pi}{6} + \alpha_1} I_d \sin n\omega t \, d\omega t \right] \quad (23.6)$$

$$= \frac{4I_d}{n\pi} \sin \frac{n\pi}{3} \cos n\alpha_1 \quad n = 1, 3, 5, \dots$$

The Fourier coefficients $a_{n\Delta}$ and $b_{n\Delta}$ of the delta winding current $i_{\Delta s}$ ($= a_{n\Delta} + j b_{n\Delta}$) are

$$a_{n\Delta} = \frac{1}{\pi} \int_0^{2\pi} i_{\Delta s}(t) \cos n\omega t \, d\omega t$$

$$= \frac{2}{\pi} \left[\int_{\frac{\pi}{3} + \alpha_2}^{\frac{2\pi}{3} + \alpha_2} \frac{I_d}{3} \cos n\omega t \, d\omega t + \int_{\frac{2\pi}{3} + \alpha_2}^{\frac{\pi}{3} + \alpha_2} \frac{2I_d}{3} \cos n\omega t \, d\omega t \right. \quad (23.7)$$

$$\left. + \int_{\frac{2\pi}{3} + \alpha_2}^{\frac{\pi}{3} + \alpha_2} \frac{I_d}{3} \cos n\omega t \, d\omega t \right]$$

$$= \frac{2I_d}{3n\pi} \left[-\sin n\alpha_2 - \sin n\left(\frac{\pi}{3} + \alpha_2\right) + \sin n\left(\frac{2\pi}{3} + \alpha_2\right) + \sin n(\pi + \alpha_2) \right]$$

$$b_{n\Delta} = \frac{1}{\pi} \int_0^{2\pi} i_{\Delta s}(t) \sin n\omega t \, d\omega t$$

$$= \frac{2}{\pi} \left[\int_{\frac{\pi}{3} + \alpha_2}^{\frac{2\pi}{3} + \alpha_2} \frac{I_d}{3} \sin n\omega t \, d\omega t + \int_{\frac{2\pi}{3} + \alpha_2}^{\frac{\pi}{3} + \alpha_2} \frac{2I_d}{3} \sin n\omega t \, d\omega t + \int_{\frac{\pi}{3} + \alpha_2}^{\frac{2\pi}{3} + \alpha_2} \frac{I_d}{3} \sin n\omega t \, d\omega t \right] \quad (23.8)$$

$$= \frac{2I_d}{3n\pi} \left[\cos n\alpha_2 + \cos n\left(\frac{\pi}{3} + \alpha_2\right) - \cos n\left(\frac{2\pi}{3} + \alpha_2\right) - \cos n(\pi + \alpha_2) \right]$$

$$n = 1, 3, 5, \dots$$

The Fourier coefficients for the line current are then defined by

$$a_n = \frac{1}{2} a_{nY} + \frac{1}{2} a_{n\Delta} \quad (23.9)$$

$$b_n = \frac{1}{2} b_{nY} + \frac{1}{2} b_{n\Delta}$$

From which the input line current is defined by

$$i_a(t) = \sum_{n=1,2,3,\dots}^{\infty} \sqrt{2} I_{an} \sin(n\omega t + \varphi_n) \quad (23.10)$$

Output voltage

The converter outputs are series connected, hence the output voltage is additive for each pole, namely $V_{dr} = V_{dr1} + V_{dr2}$. The converter output voltage, with the constraint that both converters have a trigger delay of α , is

$$V_{dr} = V_{dr1} + V_{dr2} = \frac{6\sqrt{2}}{\pi N} V_{LL} \cos \alpha = 2.70 \frac{V_{LL}}{N} \cos \alpha \quad (23.11)$$

The peak output voltage occurs midway between the peak voltage from each converter, and for $\alpha = 0$

$$\hat{V}_{dr} = 2\sqrt{2} \frac{V_{LL}}{\pi N} \cos 15^\circ = 1.932\sqrt{2} \frac{V_{LL}}{\pi N} \quad (23.12)$$

Each converter delivers six current blocks of magnitude I_d , comprised of two $\frac{2}{3}\pi$ current blocks π radians apart in each converter arm. Since each converter output is the same but shifted by $\frac{1}{6}\pi$ radians, provided the two converters have equal delay angles, the resultant 12 current block per cycle results in the dc side voltage harmonics in V_{dr} being of the order $12n$.

If the two delay angles are controlled individually, the two outputs add but with harmonic components given by two six pulse converter, displaced by $\frac{1}{6}\pi$, where

$$V_{dr1} = \frac{3V_{\max}}{\pi} \left(\cos \alpha_1 + \sum_{n=1}^{\infty} \frac{1}{\sqrt{(6n-1)^2 + 1}} - \frac{2 \cos 2\alpha_1}{(6n-1)(6n+1)} \sin(6n\omega t + \lambda_{6n1}) \right) \quad (23.13)$$

$$V_{dr2} = \frac{3V_{\max}}{\pi} \left(\cos \alpha_2 + \sum_{n=1}^{\infty} \frac{1}{\sqrt{(6n-1)^2 + 1}} - \frac{2 \cos 2\alpha_2}{(6n-1)(6n+1)} \sin(6(n\omega t - \frac{1}{6}\pi) + \lambda_{6n2}) \right)$$

where

$$\lambda_{6n1} = -n\pi + \tan^{-1} \left[\frac{\cos(6n+1)\alpha_1}{(6n+1)} - \frac{\cos(6n-1)\alpha_1}{(6n-1)} \right]$$

$$\lambda_{6n2} = -n\pi + \tan^{-1} \left[\frac{\sin(6n+1)\alpha_1}{(6n+1)} - \frac{\sin(6n-1)\alpha_1}{(6n-1)} \right]$$

$$\lambda_{6n2} = -n\pi + \tan^{-1} \left[\frac{\cos(6n+1)\alpha_2}{(6n+1)} - \frac{\cos(6n-1)\alpha_2}{(6n-1)} \right]$$

$$\lambda_{6n2} = -n\pi + \tan^{-1} \left[\frac{\sin(6n+1)\alpha_2}{(6n+1)} - \frac{\sin(6n-1)\alpha_2}{(6n-1)} \right]$$

When the two delays angles differ, $\alpha_1 \neq \alpha_2$, the output voltage harmonics occur at order $6n$.

The dc link ripple current depends on the total dc link inductance L_T and the ripple magnitude varies with the rectifier and inverter converter firing angles, α_r and α_i . Provided the minimum link current is greater than the ripple magnitude, each 12-pulse converter contributes a component given by

$$I_{d \min} > I_{d \text{ ripple}} = \frac{3}{\pi} \frac{\sqrt{2} V_{LL}}{\omega L_T} 0.023 \sin \hat{\alpha}$$

The total ripple current is the sum of the connected converter component. Each converter can be operating at a different frequency, ω , be connected to different line voltages V_{LL} , and be operating in different modes so is operating at different delay angles, α .

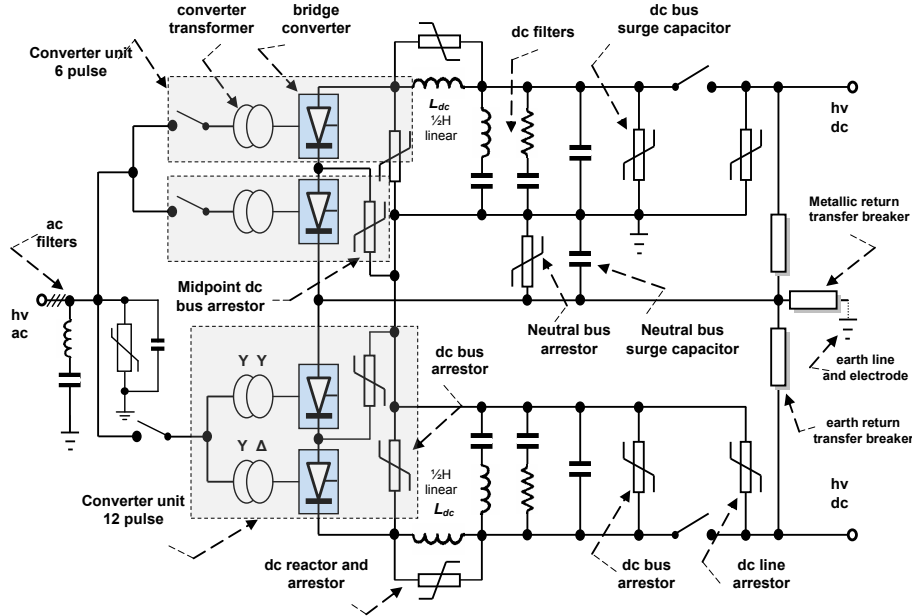


Figure 23.7. Thyristor HVDC station.

23.4.1 Rectifier mode

Figure 23.11b shows that the angle between the input ac voltage and its fundamental current I_{a1} is determined by and equals the phase delay angle α_r . The phasor diagram for rectification is shown in figure 23.12a. For a constant link current I_d , the fundamental ac input power factor is $\cos \alpha_r$ while the input reactive power is given by

$$\begin{aligned} Q_r &= \sqrt{3} V_{LL} I_{a1} \sin \alpha_r = P_r \tan \alpha_r \\ &= \sqrt{3} V_{LL} \times \frac{2\sqrt{6}}{N\pi} I_d \times \sin \alpha_r = 2.7 \times V_{LL} \times \frac{I_d}{N} \times \sin \alpha_r \end{aligned} \quad (23.14)$$

The rms of the fundamental line current I_{a1} is $2\sqrt{6}I_d / N\pi$.

The real power transfer, which is the rectifier output power, is given by

$$\begin{aligned} P_r &= V_d I_d = \sqrt{3} V_{LL} I_{a1} \cos \alpha_r = Q_r / \tan \alpha_r \\ &= \sqrt{3} V_{LL} \times \frac{2\sqrt{6}}{N\pi} I_d \times \cos \alpha_r = 2.7 \times V_{LL} \times \frac{I_d}{N} \times \cos \alpha_r \end{aligned} \quad (23.15)$$

To maximize the power flow and minimize the reactive power, the delay angle α_r should be small. From equation (23.15), to minimize the link I^2R loss, both I_d and the delay angle α_r should be small. That is, from equation (23.11), the rectifier output voltage should be maximised.

A low converter firing angle minimises the reactive power, reduce snubber losses, and reduces the harmonic content.

23.4.2 Inverter mode

The same basic rectifier mode equations hold in the inversion mode except that $\alpha_i > \frac{1}{2}\pi$. Operational waveforms and the phasor diagram for this mode are shown in figure 23.12b. The reactive power is

$$\begin{aligned} Q_i &= \sqrt{3} V_{LL} I_{a1} \sin \alpha_i = \sqrt{3} V_{LL} \times \frac{2\sqrt{6}}{N\pi} I_d \times \sin \alpha_i = 2.7 \times V_{LL} \times \frac{I_d}{N} \times \sin \alpha_i \\ &= P_i \tan \alpha_i \end{aligned} \quad (23.16)$$

and the real power transfer, which is inverted into the ac system is given by

$$\begin{aligned} P_i &= V_d I_d = \sqrt{3} V_{LL} I_{a1} \cos \alpha_i = \sqrt{3} V_{LL} \times \frac{2\sqrt{6}}{N\pi} I_d \times \cos \alpha_i = 2.7 \times V_{LL} \times \frac{I_d}{N} \times \cos \alpha_i \\ &= Q_i / \tan \alpha_i \end{aligned} \quad (23.17)$$

To maximize the ac system power and minimize the reactive power, the delay angle α_i should be large ($\rightarrow \pi$). From equation (23.17), to minimise the link I^2R loss, I_d should be minimised (maximise dc link voltage) and the delay angle α_i should be large ($\rightarrow \pi$). Thus the inversion voltage should be as large as possible, avoiding commutation failure. Then the maximum α_i decreases as current increases since thyristor commutation time increases with current (and temperature).

P-Q operation of the twelve pulse series connected converter

The theory of controlled active and reactive power operation of a series connected 12-pulse converter assumes an ideal input transformer, negligible source impedance, and a constant current from the converter dc output bus. The output voltage contribution due to each constituent 6-pulse converter is given by

$$V_{a1} = \frac{3V_{max}}{\pi} \cos \alpha_i \quad (23.18)$$

where V_{max} is the peak line voltage of the voltage applied to each converter, α_i is the firing angle of the constituent converter, and i represents either converter 1 or 2.

By multiplying (23.18) by the dc load current I_{dc} , the active power is given by

$$Q_i = P_{max} \sin \alpha_i \quad (23.19)$$

where

$$P_{max} = \frac{3}{\pi} I_{dc} V_{max}$$

which represents the maximum power delivered from each converter at $\alpha_i = 0$. Similarly, the reactive power absorbed by the converter is given by

$$Q_i = P_{max} \sin \alpha_i \quad (23.20)$$

The active power P_d and reactive power Q_d , drawn by the 12-pulse converter are the sum of the contribution made by each converter, namely

$$\begin{aligned} P_d &= P_{max} (\cos \alpha_1 + \cos \alpha_2) \\ Q_d &= P_{max} (\sin \alpha_1 + \sin \alpha_2) \end{aligned} \quad (23.21)$$

From these two equations, the 12-pulse converter draws active power of $2P_{max}$ and zero reactive power at $\alpha_1 = \alpha_2 = 0$. Similarly, at $\alpha_1 = \alpha_2 = \frac{1}{2}\pi$, the converter draws reactive power of $2P_{max}$ and zero active power. Therefore, $2P_{max}$ is the base power, 1 pu, and the equations in (23.21) become

$$\begin{aligned} P_{pu} &= \frac{1}{2} (\cos \alpha_1 + \cos \alpha_2) \\ Q_{pu} &= \frac{1}{2} (\sin \alpha_1 + \sin \alpha_2) \end{aligned} \quad (23.22)$$

The variation of P_{pu} and Q_{pu} with simultaneous variation of α_1 and α_2 is shown in the three-dimensional plots figure 23.8.

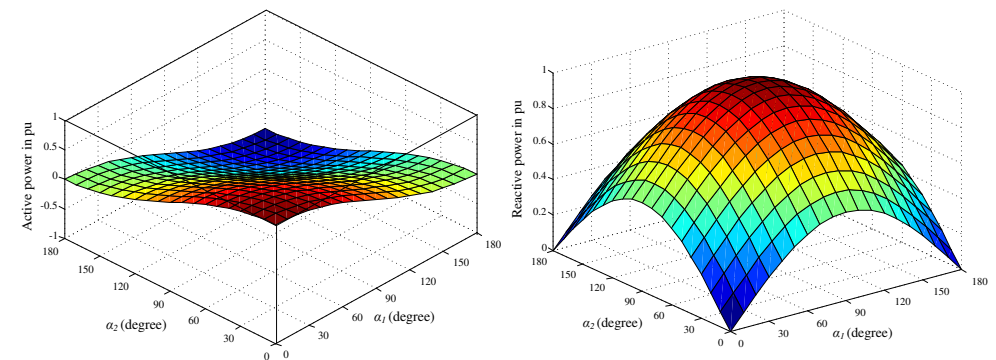


Figure 23.8. Effects of varying of α_1 and α_2 on: (a) active power and (b) reactive power.

The 12-pulse converter may operate with symmetrical firing of each 6-pulse converter, where $\alpha_1 = \alpha_2$ or with asymmetrical firing where $\alpha_1 \neq \alpha_2$ (or a combination of both). Different power loci can be realized by different combinations of firing angles (α_1 and α_2). Three power loci are shown in part 'a' of figure 23.9. The symmetrical firing P - Q locus is represented by the outer semicircle with centre '0' and radius of 1 pu, and is obtained by the symmetrical firing of α_1 and α_2 from 0 to π using the parts of equation (23.22). All points in the P - Q plane within the outer semicircle can be achieved by unique combinations of α_1 and α_2 . The figure also shows power loci for asymmetrical firing which are represented by the circumference of the two inner semicircles with radii of 0.5 pu. These are obtained by varying α_1 from 0 to π while α_2 is held at '0' in the case of rectification and by varying α_2 from 0 to π while α_1 is held at π in the case of inversion. Part 'a' also shows the power locus for constant VAR operation indicated by the line parallel to the P -axis. With asymmetrical firing the maximum reactive power is decreased to one-half the case for symmetrical firing. Part 'b' of figure 23.9 shows the variation of input current THD with varied delay angles and reflects the adverse effect of asymmetrical firing on the THD.

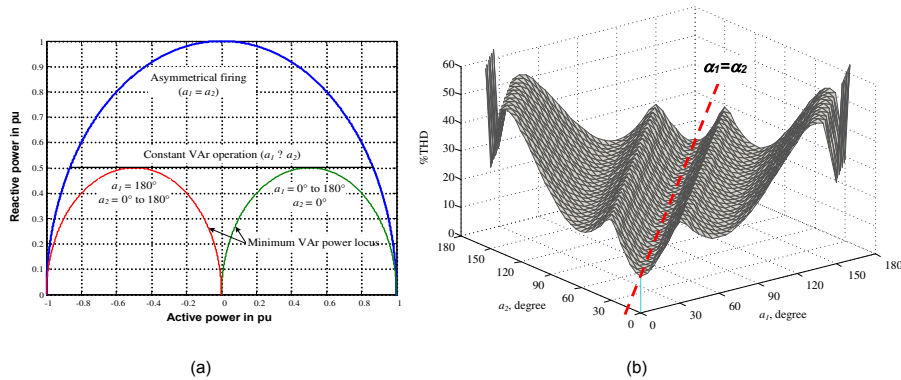


Figure 23.9: Twelve-pulse fully-controlled converter: (a) power loci and (b) input current THD.

The symmetrical firing power locus is associated with the best THD and the worst supply current power factor. On the other hand, asymmetrical firing decreases the reactive power flowing in the system, which improves the input power factor but deteriorates the input current THD, which limits the power factor improvement. As a result, asymmetrical firing of the 12-pulse converter offers the possibility of a smaller reactive power compensator for power factor compensation, at the expense increased input current harmonics.

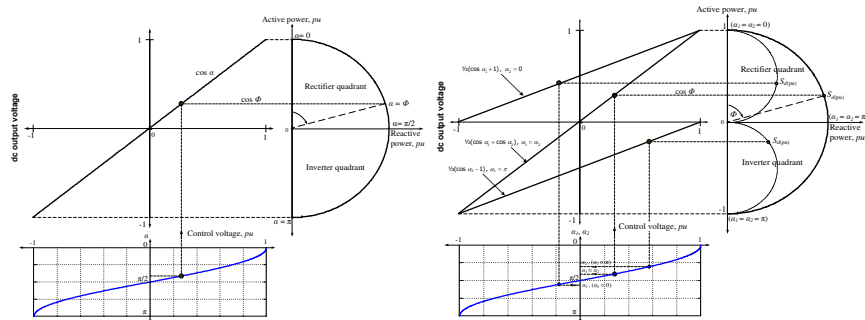


Figure 23.10: Power locus of 6-pulse and 12-pulse converters and per unit output voltage.

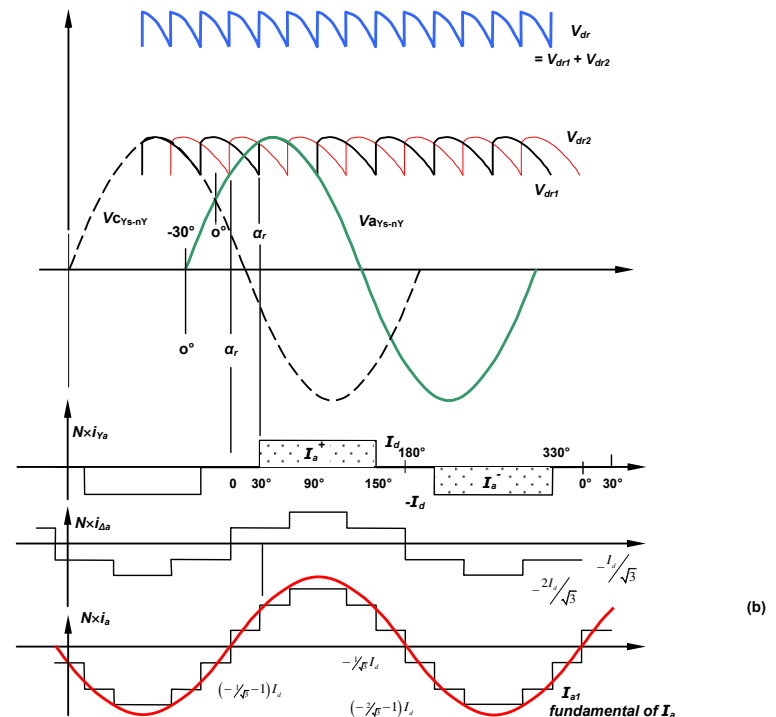
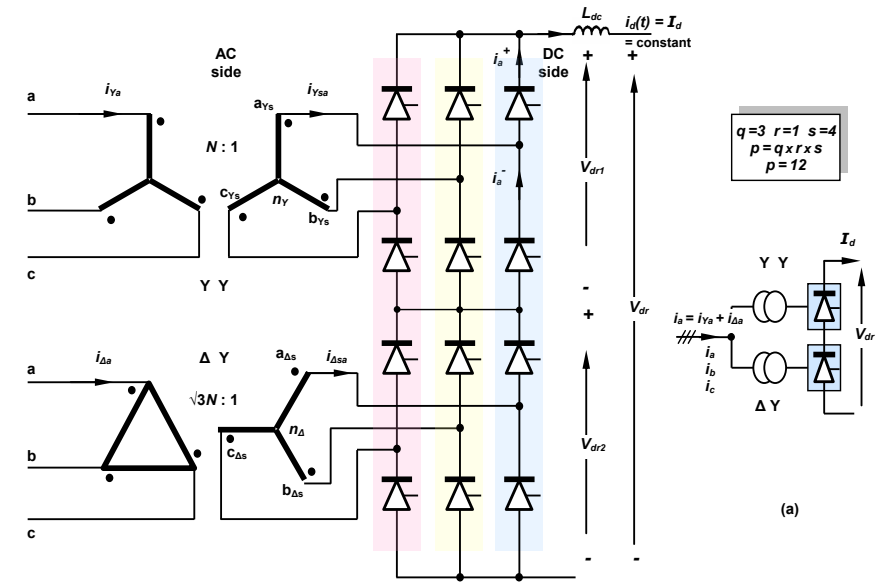


Figure 23.11: Twelve-pulse valve group converter configuration with star-star and star-delta connected converter transformers: (a) converter schematic and (b) twelve-pulse valve group waveforms.

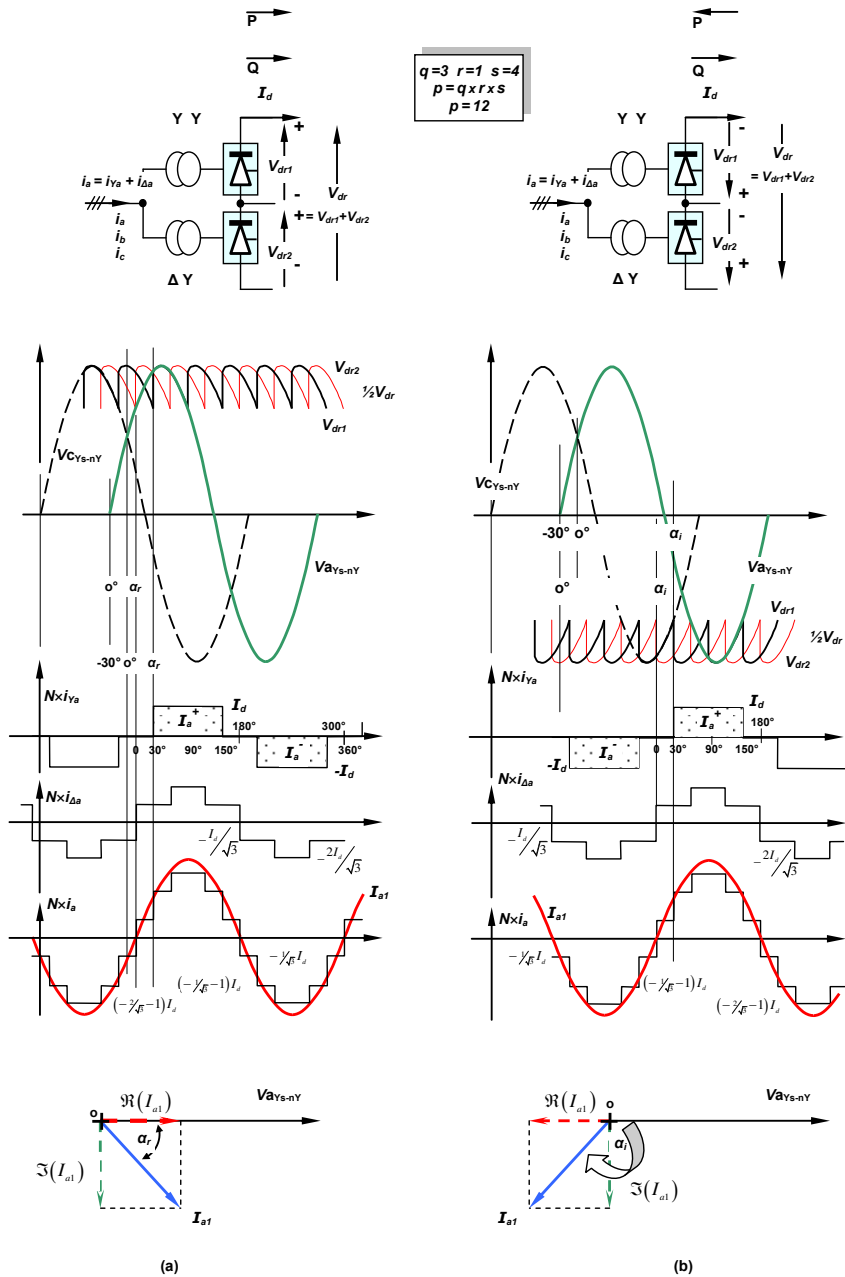


Figure 23.12. Twelve-pulse valve group converter configuration with star-star and star-delta connected converter transformers operating in: (a) a rectifying mode and (b) an inverting mode.

23.5 Twelve-pulse ac line frequency converter operation control

Rectification and inversion modes of converter operation and the line (or natural) commutation process of the three-phase fully-controlled thyristor converter have been considered in chapter 14.4 for rectification, with overlap in 14.5, and 14.6 for inversion with overlap.

One converter operates as a rectifier (power flow from ac to dc) and the other dc link converter operates as an inverter (power flow from dc to ac). Either terminal converter can operate as an inverter or rectifier, since the delay angle determines the mode (voltage) of operation. The power flow between the two ac systems connected to the HVDC link is controlled by controlling the delay angle of each converter. Current only flows in one direction in the dc link, from the rectifier to the inverter. A simple system model is shown figure 23.13 where the link dc resistance is represented by R_{dc} and source reactance, hence overlap effects have been neglected. Let the transformer turns ratio factor N equal 1. The dc current I_d is

$$I_d = \frac{V_{dr} + V_{di}}{R_{dc}} \tag{23.23}$$

where

$$V_{dr} = \frac{3}{\pi} \sqrt{2} V_{LL} \cos \alpha_r \text{ for } 0 \leq \alpha_r \leq \frac{1}{2}\pi$$

$$V_{di} = \frac{3}{\pi} \sqrt{2} V_{LL} \cos \alpha_i \text{ for } \frac{1}{2}\pi \leq \alpha_i \leq \pi$$

$$\tag{23.24}$$

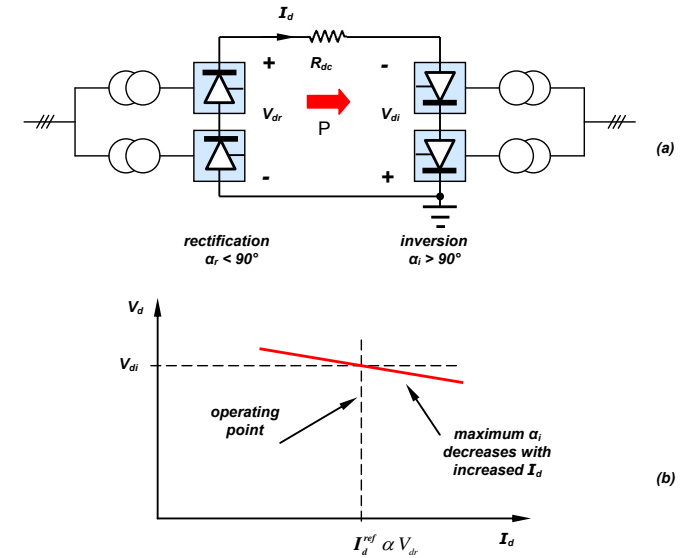


Figure 23.13. Basic HVDC transmission system: (a) circuit diagram and (b) load line characteristics.

The rectifier output power is

$$P_r = V_{dr} I_d \tag{23.25}$$

while the power supplied to the inverter is

$$P_i = V_{di} I_d \tag{23.26}$$

where

$$P_r = V_{dr} I_d = V_{di} I_d + I_d^2 R_{dc} = P_i + I_d^2 R_{dc} \tag{23.27}$$

If transformer per phase leakage inductance L_s , referred to the converter side, is accounted for, then the resultant overlap at commutation reduces the output voltage for each six-pulse converter.

$$V_{dr} = 2 \times \left(\frac{3}{\pi} \sqrt{2} V_{LL} \cos \alpha_r - \frac{3\omega L_s}{\pi} I_d \right) = \frac{6}{\pi} \times \left(\sqrt{2} V_{LL} \cos \alpha_r - \omega L_s I_d \right) \tag{23.28}$$

Both the rectifier and inverter dc output voltages can be compensated for leakage reactance commutation overlap. Remember the overlap voltage component is not a loss element in the resistor sense. It represents a 'lossless' loss of voltage which increases with current.

If the link voltage is controlled by the inverter and the dc current controlled by the rectifier, then the load line characteristic in figure 23.13c results. The inverter voltage is kept slightly below the rectifier voltage. As the load current increases, the inverter terminal voltage is reduced. This is because the time to safely commutate the inverter thyristors increases with current, hence α_i must decrease, as shown by the droop in the output characteristics in figure 23.13b. The more detailed practical approach to HVDC power transport control is considered in section 23.5.1.

23.5.1 Control and protection

HVDC transmission systems must operate under tightly controlled conditions. Dc-link current and the two terminal voltages are precisely controlled to affect the desired power transfer. Accurate system quantity measurements are required, which include at each converter bridge, the dc-link current, the dc-side voltages, and the delay angle α for each converter/inverter.

Two terminal dc transmission systems have a preferred control mode during normal operation.

Inverter

Under steady-state conditions, the inverter controls the dc voltage by one of two methods.

- The inverter maintains a constant delay angle $\alpha_i > 90^\circ$, or extinction angle γ , where $\gamma = \pi - \alpha_i$. This constant angle maintenance causes the dc voltage V_d to droop with increasing dc current I_d , as shown in the minimum constant extinction angle $\check{\gamma}$ characteristic in figure 23.14b and labelled A-B-C-D in figure 23.14c. The weaker the ac system at the inverter, the steeper the droop characteristic.
- Alternatively, the inverter may operate in a dc voltage controlling mode which is the constant V_d characteristic shown dashed in figure 23.14b and labelled B-H-E in figure 23.14c. To achieve this, the extinction angle γ must increase beyond its minimum value characterised in figure 23.14b as $\check{\gamma}$.

Rectifier

If the inverter is operated in either a minimum constant γ or constant V_d mode, then the rectifier is used to control the dc link current I_d . This is achievable provided the delay angle α_r is not at its minimum limit. The steady-state constant current characteristic of the rectifier is shown in figure 23.14a as the vertical section of the characteristic S-T and is labelled S-C-H-T in figure 23.14c. The rectifier delay angle is increased toward $\alpha_r = 90^\circ$ if the link current attempts to increase beyond the reference level I_d^{ref} . During an attempted short circuit fault, the rectifier delay angle reaches 90° which sets the rectifier output voltage to zero, as shown by equation (23.24), and controls the fault current to I_d^{ref} as shown by trajectory S-T in figure 23.14a.

The operating point of the HVDC system is where the rectifier characteristic intersects the inverter characteristics, either at point C or point H on figure 23.14c, depending on which of the two inverter control methods is being employed. The operating point is tuned over a period of tens of seconds by adjusting the line-side tap changers of the converter transformers.

The inverter controls the dc-link voltage as follows.

- The inverter establishes the desired dc voltage V_d by tap changer adjustment, if it is operated in a constant minimum γ mode.
- If the inverter is operated in a constant V_d mode, the tap changer is adjusted to produce constant V_d with an extinction angle slightly larger than the minimum $\check{\gamma}$.

The ac-side tap changers on the rectifier end transformers are adjusted so that the delay angle α is small but with a 5° working range, whilst maintain the constant current I_d^{ref} . If the inverter is constant dc voltage operated at the operating point H, and if the dc current I_d^{ref} is increased so that the operating point H moves towards A, the inverter control mode reverts to constant extinction angle γ control when operating in the droop region A-B. The voltage V_d droops to less than the desired value, so the inverter end transformer tap changer progressively boosts the dc-side voltage until dc voltage control recommences, in region B-C-D.

Not all HVDC transmission systems use constant dc voltage control, which is the horizontal characteristic B-H-E in figure 23.14c. Instead, the tap changer in conjunction with the constant extinction angle γ control characteristic A-B-C-D in figure 23.14c, provides dc voltage control.

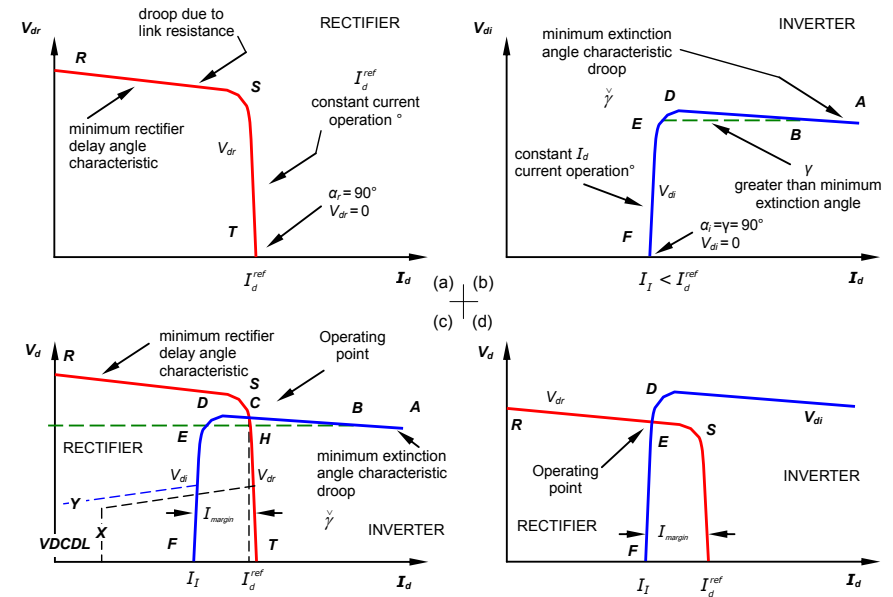


Figure 23.14. Steady-state $V_d - I_d$ characteristics for a two terminal HVDC system.

Current margin

The rectifier and inverter controllers both receive the dc current demand I_d^{ref} but the inverter current demand is decreased by an amount termed the current margin I_{margin} , as shown in Figure 23.14c. This current margin is usually a constant magnitude of about 10% of rated current. The inverter current controller endeavours to control the dc link current to $I_i = I_d^{ref} - I_{margin}$ but the rectifier current controller dominates and maintains the dc current at I_d^{ref} . In steady-state the rectifier controller overrides the inverter controller which is not able maintain a dc current $I_d^{ref} - I_{margin}$. The inverter current controller only becomes active when the rectifier current controller has reduced its delay angle α_r to the minimum limit. This rectifier minimum delay angle limit is characterised by R-S in figure 23.14c.

Control characteristic performance

Variations in the ac voltages change the control operating point of the system as follows.

- When the rectifier side ac voltage decreases and/or the inverter side ac voltage increases, then the transformer tap adjustment mechanisms on both the rectifier and inverter transformers should attempt to remedy this ac voltage regulation problem. If the disturbance is large enough, the new stable operating point is shown in figure 23.14d. The R-S characteristic falls below points D or E, the operating point will shift from point H to somewhere on the vertical characteristic D-E-F where it is intersected by the lowered minimum α_r R-S characteristic as shown in figure 23.14d. The inverter converts to current control, controlling the dc current I_d to the value $I_i = I_d^{ref} - I_{margin}$, approximately 10% of rated current and the rectifier effectively controls the dc voltage provided it is operating at its minimum delay angle characteristic R-S. The dc power flow is relatively unaffected and safely returns to the normal operating condition shown in figure 23.14c, once the ac disturbances have subsided.
- If the rectifier ac voltage increases, the reference current, which is set by the rectifier, is unaffected. Since the link voltage is set by the inverter, any increase in rectifier ac voltage does not affect the power flow. This can be seen in figure 23.14c where increasing the rectifier characteristic R-S does not affect the intersection of the operating point C, whence power flow is unaffected by an increase in the rectifier ac-side voltage.
- If the inverter side ac voltage is decreased, the link voltage decreases proportionally, but the current is unaffected because it is set by the rectifier. The power flow is therefore decreased in line with the inverter ac voltage decrease. This can be seen in figure 23.14c where the inverter side ac voltage decrease will lower the inverter characteristic A-B-C-D. The operating point C, the operating voltage, decreases but the current is unaffected. Thus the power transferred is decreased in-line with the inverter ac-side voltage.

vi. Worst case conditions are a dc-link short circuit. As seen in figure 23.14a, the rectifier maximum current is I_d^{ref} , while figure 23.14b shows that the maximum inverter current is I_I . The maximum fault current is therefore limited to the operational current margin I_{margin} . As seen in figures 23.14a and 23.14b, the control angle of both converters moves to 90° , which produces 0V converter output voltages, as shown by equation (23.24). Hence the power associated with any short circuit fault is low, unlike short circuit faults in ac transmission systems.

Voltage dependant current demand limit (VDCDL)

If the ac voltages sag significantly because of weak ac systems, it may not be possible to maintain full load current. In such a case the dc-link voltage is decreased, and the controller characteristics are dictated by the trajectories X and Y in figure 23.14c. A controller which reduces the maximum current demand in such conditions, is termed a voltage dependant current demand limiter, or VDCDL. The current is not reduced to zero so that recovery response is faster once the dc-link voltage has sufficiently recovered.

Power flow reversal

The controllers can be designed such that the transition from the rectifier controlling current to the inverter controlling current, is automatic and smooth. That is, seamless automatic power flow reversal is achieved by interchanging the inverter and rectifier functions, as seen in figure 23.15. This is realised by appropriate control of the delay angles, hence terminal polarities, but the dc link current direction does not reverse. Such a bi-directional power flow requirement may be necessary when two ac systems are required to bi-directionally interchange power. The rectifier delay angle is progressively increased while the inverter delay angle is decreased, such that the rectifier and inverter voltage difference is control to be virtually constant. This is achieved if $\alpha_r + \alpha_i \approx 180^\circ$ is maintained.

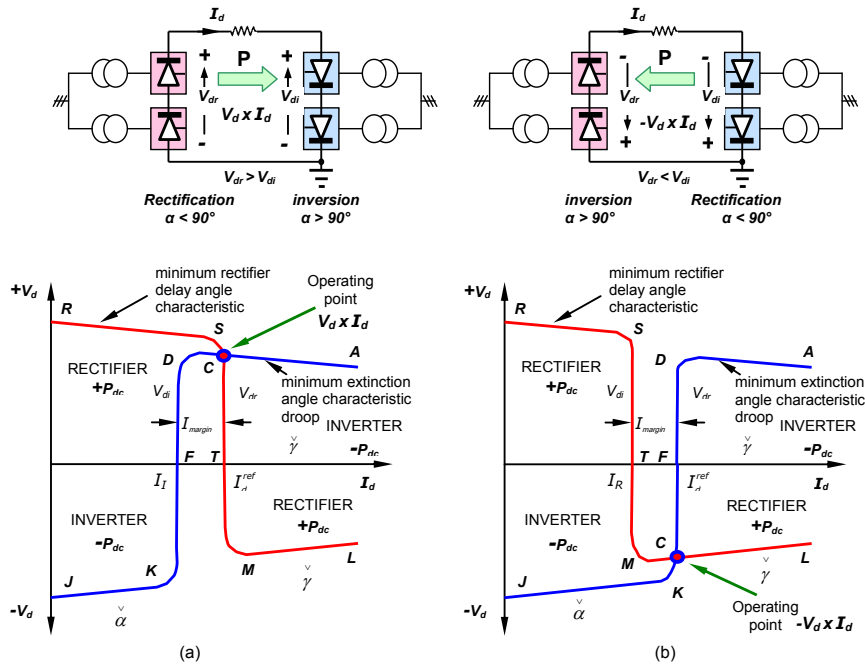


Figure 23.15. Power reversal in HVDC systems by voltage polarity reversal, not current reversal.

23.5.2 HVDC Control objectives

The fundamental objectives of a CSI-based HVDC control system are as follows:

- to control basic system quantities such as dc line current, dc voltage, and transmitted power accurately and with sufficient speed of response;

- to maintain adequate commutation margin in inverter operation so that the valves can recover their forward blocking capability after conduction before their voltage polarity reverses;
- to control higher-level parameters such as frequency in isolated mode or provide power oscillation damping to help stabilize the ac network;
- to compensate for loss of a pole, a generator, or an ac transmission circuit by rapid readjustment of power;
- to ensure stable operation with reliable commutation in the presence of system disturbances;
- to minimize system losses and converter reactive power consumption; and
- to ensure proper operation with fast and stable recovery from ac system faults and disturbances.

23.6 Delta/Delta/Double polygon 18 pulse converter

Six-pulse bridge circuits can be in series or parallel to create an 18-pulse converter. In series, as in figure 23.16, power source harmonic voltages can be eliminated. The series connection does not need inter-phase transformers, unlike parallel connected converters.

Transformer leakage inductances are an important practical feature in the design. An alternative method using physically separate phase-shifting transformers is also feasible. In principle this connection can be extended to higher pulse numbers by increasing the number of polygon windings and modifying the phase shift accordingly. Practical limitations occur due to reactance effects, efficiency, and the limit on available turns ratios. The shift angle is 360° divided by the pulse number.

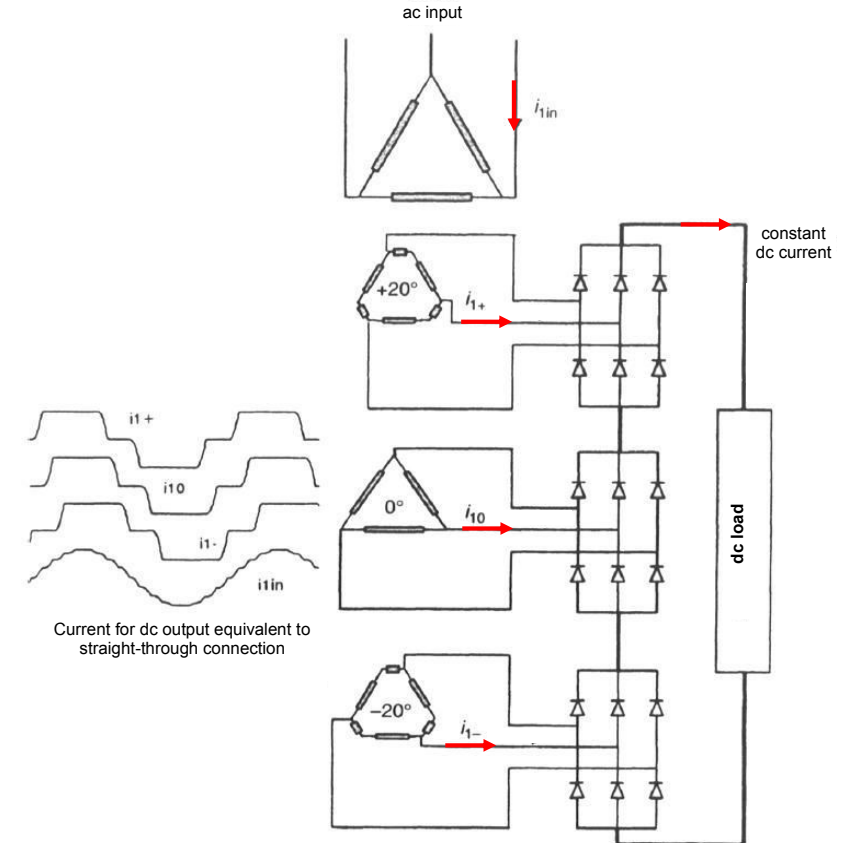


Figure 23.16. Delta/delta/double polygon for 18 pulse rectifiers.

Appropriate zig-zag and forked connections could also be employed to provide similar 18 pulse characteristics. However, polygons are easier to use for low-voltage outputs because the higher number of turns facilitates selection of the turns ratios.

23.6.1 Analysis of Double-Wound Polygon

Analysis of closed polygon connections tends to be more cumbersome than that for open (fork) connections. Thus the procedure for the general polygon case is presented.

Let ϕ be the phase shift between polygon output line-to-line voltage V_{Ls} and the delta input line-to-line voltage V_{Li} . Let the turns/phase on the delta winding be N_p and polygon windings have N_l turns for the long winding and N_s turns for the short winding. Figure 23.17 shows the arrangement for reference.

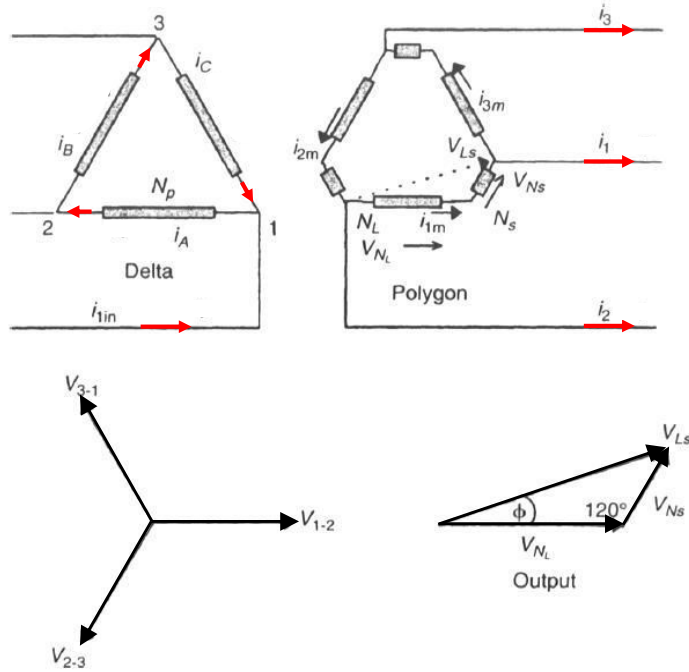


Figure 23.17. Double-wound polygon connection phasor diagram.

Polygon voltages and phase shift

From the polygon vector drawing in figure 23.17

$$\frac{V_{Ls}}{\sin 120^\circ} = \frac{V_{Ns}}{\sin \phi} = \frac{V_{Nl}}{\sin 60^\circ - \phi}$$

Thus

$$\text{polygon long winding voltage: } V_{Nl} = \frac{2}{\sqrt{3}} V_{Ls} \sin(60^\circ - \phi)$$

and

$$\text{polygon short winding voltage: } V_{Ns} = \frac{2}{\sqrt{3}} V_{Ls} \sin \phi \quad (4.2)$$

From the figure 23.17

$$\tan \phi = \frac{V_{Ns} \sin 60^\circ}{V_{Nl} + V_{Ns} \cos 60^\circ}$$

Thus for a turns ratio given by $n = V_{Nl} / V_{Ns}$

$$\phi = \tan^{-1} \frac{\sqrt{3}}{1 + 2n}$$

Polygon winding currents

$$i_{1m} - i_{3m} = i_1$$

$$i_{2m} - i_{1m} = i_2$$

Subtracting these equations gives

$$i_{1m} - i_{3m} - i_{2m} + i_{1m} = i_1 - i_2$$

Incorporate $i_{1m} + i_{2m} + i_{3m} = 0$

$$i_{1m} = \frac{i_1 - i_2}{3}$$

Also

$$i_{2m} = \frac{i_2 - i_3}{3} \text{ and } i_{3m} = \frac{i_3 - i_1}{3}$$

In general, the converter input currents consist of current pulses with amplitude I_d . They incorporate harmonics of the form $(6k \pm 1)$, which include positive-and negative-sequence currents. To calculate the rms current in the winding, these harmonics are considered individually then summed ($\sqrt{\sum I^2}$) to determine the total rms value. The fundamental and rms currents in each converter line are displaced by $\pm \pi/3$ depending on their sequence. Thus, each component, hence the total, is multiplied by

$$\left[(1 - \cos \pm \pi/3)^2 + (\sin \pm \pi/3)^2 \right]^{1/2}$$

that is, $\sqrt{3}$, as it flows into the secondary windings. The idealized converter line current is a 120° conduction square wave with rms value of $I_d \sqrt{2/3}$. Substituting these results into the equation for i_{1m} , yields

$$\text{secondary winding rms current } \sqrt{3} \frac{1}{3} \sqrt{\frac{2}{3}} I_d = 0.471 I_d$$

When load currents; i_1 , i_2 , and i_3 which are characteristic of a three-phase bridge rectifier, are present, the line input current to the delta winding is calculated as follows. The sum of ampere-turns on the transformer core must be zero. Thus

$$i_A N_p - i_{1m} N_l + i_{3m} N_s = 0$$

from which

$$i_A = i_{1m} \frac{N_l}{N_p} - i_{3m} \frac{N_s}{N_p}$$

and, similarly

$$i_C = i_{3m} \frac{N_l}{N_p} - i_{2m} \frac{N_s}{N_p}$$

The delta winding line input current is given by

$$i_{1in} = i_A - i_C$$

Thus

$$i_{1in} = \frac{N_l}{N_p} (i_{1m} - i_{3m}) + \frac{N_s}{N_p} (i_{2m} - i_{3m})$$

From Figure 23.17

$$i_{1m} - i_{3m} = i_1 \text{ and } i_{2m} - i_{1m} = i_2$$

Thus

$$i_{2m} - i_{3m} = i_1 - i_2$$

Therefore

$$i_{1in} = i_1 \left[\frac{N_l}{N_p} + \frac{N_s}{N_p} \right] + i_2 \frac{N_s}{N_p}$$

When the voltage ratio output to input is 1:1,

$$\frac{N_l}{N_p} = \sqrt{\frac{2}{3}} \text{ and } \frac{N_s}{N_p} = \frac{\sqrt{3}-1}{\sqrt{6}}$$

The phase shift is governed by the ratio of the secondary turns and is determined to be 15°.

Using these ratios, the line input current is

$$i_{1in} = 1.1153 i_1 + 0.299 i_2 \text{ for } 15^\circ$$

Extending this analysis, the polygon winding kVA can be determined in respect to the dc load power. The result is

$$\frac{\text{D.W. polygon winding VA}}{V_{do} I_d} = 1.209 (\sin(60^\circ - \phi) + \sin \phi)$$

23.7 Filtering and power factor correction

As shown in figure 23.7, both ac and dc side filtering is used to reduce radiated EMC on the dc link and conducted EMC on the ac sides which causes power losses and interference.

On the dc-side, the large link inductance at each converter (typically between $\frac{1}{5}H$ and $\frac{1}{2}H$) is supplemented with LC filters, tuned to eliminate selected $12n$ current harmonics in a 12-pulse system. A filter is notch tuned to eliminate (shunt) one specific harmonic, usually the most dominate 12^{th} . At 50/60Hz, these filters are capacitive thus provide reactive power absorbed by the converters. Harmonics occur at $12n \pm 1$ on the ac-side. Again, tuned LC filters eliminate (shunt) specific low order harmonics and a general high pass shunt filter is used for components above the 11^{th} and 13^{th} . Generally, higher pulse order (>12) transformer/converter arrangements are not attractive in HVDC because of the difficulties in producing high-voltage transformers (auto-transformers tend to be used). Additional to the VAR compensation provided by the ac harmonic filters, pure capacitance may also be used. In order to avoid overcompensation voltage regulation problems which can occur at low power transmission levels, the extra capacitance tends to be switched in-circuit as needed.

The main transformers may be provided with ac-side voltage taps to adjust the secondary voltage, as considered in section 23.5.1. The taps are switched automatically by motorised tap-changing drives, which only operate when large voltage changes occur for prolonged periods of time. If the transformers have only Y-Y winding configurations, they may also have a low-voltage delta tertiary winding for VAR compensation, provide ancillary supplies, and suppression of transformer core triplen harmonic fluxes.

Feature summary of Line Commutated Thyristor Systems

With the exception of multi-terminal HVDC the basic steady state operation required of FACTS and HVDC systems may be achieved through the use of thyristor based systems. There are however limits on the performance and functionality that may be achieved.

Advantages

- High voltage thyristor devices give low losses and are available in robust high-current capacity single-wafer capsules that fail short circuit.
- Line commutated HVDC and FACTS have an established track record at transmission voltage and power levels.

Disadvantages

- Line commutated systems inject significant low frequency harmonics which must be eliminated by large (physically and electrically) passive filter arrangements. The presence of these filters may lead to circulating harmonic currents which must be mitigated by damping networks. Filters and damping networks may have to be designed specifically for each location and may not be optimal for all operating conditions.
- Line commutated systems are inherently limited in response time (limited to line frequency switching) and may suffer control capability limits. For example thyristor based HVDC:
 - cannot decouple the real and reactive power injected into the network.
 - may have limited operating range depending on the source impedance provided by the ac network at the point of connection.
- Line commutated circuits tend to require large passive components leading to large footprint systems.

Example 23.1: Basic six-pulse converter based hvdc transmission

The basic six-pulse converter dc transmission system represented by figure 23.18 connects a 230kV ac rms, 50Hz system to a 220kV, 60Hz system. The 6-pulse converters at each transmission line end are interface by a Δ_{ac} - Y_{dc} transformers of turns ratio $\sqrt{3}:2$, as shown, such that the transformer dc-side line voltage is double the ac side line voltage. The power transmission is 500MW to the inverter which is maintained at a dc voltage level of 500kV. The total dc-link resistance is 8Ω .

Determine

- The inverter delay angle, α_i .
- The dc-link current, hence rectifier output voltage, thence rectifier delay angle, α_r .
- The rectifier input power and VAR, and inverter VAR, thence system efficiency.

Solution

Because of the transformer turns ratio, the transformer dc-side ac voltages are double the ac-side voltages.

- The inverter delay angle is derived from equation (23.24)

$$V_{di} = \frac{3}{\pi} \sqrt{2} V_{Ll} \cos \alpha_i$$

$$500kV = \frac{3}{\pi} \sqrt{2} \times 2 \times 220kV \times \cos \alpha_i$$

that is $\alpha_i = 147.3^\circ$

- From $P_i = V_{di} \times I_d$, the link current is

$$I_d = \frac{500 \times 10^6 \text{ W}}{500 \times 10^3 \text{ V}} = 1000 \text{ A}$$

The rectifier output voltage is given by equation (23.23), rearranged

$$V_{dr} = -V_{di} + I_d R_{dc}$$

$$= -500kV + 1000A \times 1\Omega = 508kV$$

The rectifier delay angle is derived from equation (23.24)

$$V_{dr} = \frac{3}{\pi} \sqrt{2} V_{Ll} \cos \alpha_r$$

$$508kV = \frac{3}{\pi} \sqrt{2} \times 2 \times 230kV \times \cos \alpha_r$$

yields $\alpha_r = 35^\circ$

- The input power is the output plus dc-link resistive losses, that is

$$P_r = I_d^2 \times R_{dc} + P_i$$

$$= 1000^2 \times 8\Omega + 500MW = 508MW$$

The input VAR from the ac side is

$$Q_r = P_r \tan \alpha_r$$

$$= 508MW \times \tan 35^\circ = 355.7MVAR$$

Similarly, the inverter VAR into the ac side (indicated by the negative sign) is

$$Q_i = P_i \tan \alpha_i$$

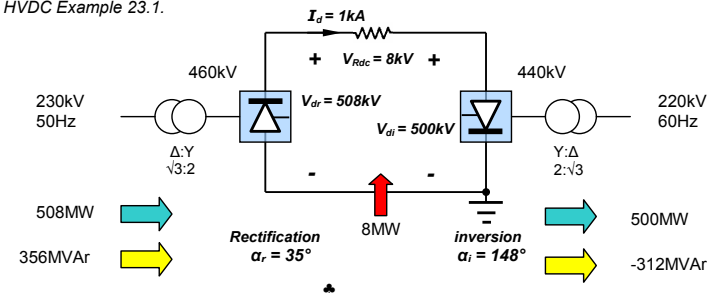
$$= 500MW \times \tan 148^\circ = -312.4MVAR$$

The efficiency is

$$\eta = \frac{P_i}{P_o}$$

$$= \frac{500MW}{508MW} \times 100 = 98.43\%$$

Figure 23.18. HVDC Example 23.1.



The following example is based on example 23.1.

Example 23.2: 12-pulse hvdc transmission

The dc transmission line represented by figure 23.13 connects a 230kV ac rms, 50Hz system to a 220kV, 60Hz system. The 12-pulse bipolar converters at each transmission line end are interface by a Y-Y transformer of turns ratio 1:1 and a Δ-Y transformer of turns ratio 1:√3, each with a converter side inductance of 1mH. The rectifier delay angle is $\alpha = 30^\circ$ for 500MW power transmission and the inverter advance angle is $\alpha = 160^\circ$ (in order to avoid any reactive power increase), which maintains the dc voltage level at 500kV at the inverter end.

The total line resistance is 8Ω and the dc link smoothing inductance is large enough to initially consider the dc current to be ripple free.

Determine

- The transformer tap ratios at each end, the dc link efficiency, I^2R losses, and both terminal VAR
- If the rectifier tap ratio of 0.866 results in the transmission current limit giving a power of 600MW, find the delay angle and line efficiency for 500kV at the inverter.
- The value of the dc link inductance L_{dc} such that the link peak to peak current is 0.1pu the average load current at full load (1200A), assuming the normalised magnitude of the dc side harmonic V_{12} is 0.15pu maximum (with respect to the 50Hz supply).

Solution

- From $P_i = V_{di} \times I_d$, the link current is

$$I_d = \frac{500 \times 10^6 \text{ W}}{500 \times 10^3 \text{ V}} = 1000 \text{ A}$$

The inverter voltage, accounting for the transformer tapping a_i is given by an equation similar to equation (23.28), that is

$$V_{di} = 2 \times \left(\frac{3}{\pi} \sqrt{2} a_i V_{LL} \cos \alpha_r - \frac{3\omega L_s}{\pi} I_d \right)$$

$$500 \times 10^3 \text{ V} = 2 \times \left(\frac{3}{\pi} \sqrt{2} a_i 220 \times 10^3 \text{ V} \cos(180^\circ - 160^\circ) - \frac{3 \times 2 \times \pi \times 60 \text{ Hz} \times 1 \times 10^{-3} \text{ H}}{\pi} 1000 \text{ A} \right)$$

which gives a transformer tap ratio at the inverter end of $a_i = 0.896$.

From equation (23.23), the rectifier voltage is

$$\begin{aligned} V_{dr} &= V_{di} + R_{dc} I_d \\ &= 500 \text{ kV} + 8 \Omega \times 1000 \text{ A} = 508 \text{ kV} \end{aligned}$$

and the necessary transformer tap ratio a_r is derive from

$$V_{dr} = 2 \times \left(\frac{3}{\pi} \sqrt{2} a_r V_{LL} \cos \alpha_r - \frac{3\omega L_s}{\pi} I_d \right)$$

$$508 \times 10^3 \text{ V} = 2 \times \left(\frac{3}{\pi} \sqrt{2} a_r 230 \times 10^3 \text{ V} \cos 30^\circ - \frac{3 \times 2 \times \pi \times 50 \text{ Hz} \times 1 \times 10^{-3} \text{ H}}{\pi} 1000 \text{ A} \right)$$

which gives a transformer tap ratio at the rectifier end of $a_r = 0.945$.

The link efficiency is

$$\begin{aligned} \eta &= \frac{P_i}{P_r} \times 100 = \frac{V_i I_d}{V_r I_d} \times 100 \\ &= \frac{500 \text{ kV}}{508 \text{ kV}} \times 100 = 98.4\% \end{aligned}$$

The I^2R losses are $1000\text{A}^2 \times 8\Omega = 8\text{MW}$ or $(508-500)^2/8\Omega$, dissipated, distributed along the line.

The rectifier reactive power is given by equation (23.14), that is

$$\begin{aligned} Q_r &= P_r \tan \alpha_r \\ &= (500 \text{ MW} + 1000\text{A}^2 \times 8\Omega) \times \tan 30^\circ = 293.3 \text{ MVAR} \end{aligned}$$

This is 293.3MVAR from to rectifier ac side.

The inverter reactive power is given by equation (23.16), that is

$$\begin{aligned} Q_i &= P_i \tan \alpha_i \\ &= 500 \text{ MW} \times \tan 160^\circ = -182 \text{ MVAR} \end{aligned}$$

This is 182MVAR to the ac side of the inverter.

- At 500kV and 600MW:

$$I_d = \frac{P_i}{V_{di}} = \frac{600 \text{ MW}}{500 \text{ kV}} = 1200 \text{ A}$$

Accounting for the link resistive voltage drop

$$\begin{aligned} V_{dr} &= V_{di} + R_{dc} I_d \\ &= 500 \text{ kV} + 8 \Omega \times 1200 \text{ A} = 509.6 \text{ kV} \end{aligned}$$

The efficiency is

$$\begin{aligned} \eta &= \frac{P_i}{P_r} \times 100 = \frac{V_i I_d}{V_r I_d} \times 100 \\ &= \frac{500 \text{ kV}}{509.6 \text{ kV}} \times 100 = 98.1\% \end{aligned}$$

The necessary rectifier angle, accounting for transformer reactive inductance, is

$$V_{dr} = 2 \times \left(\frac{3}{\pi} \sqrt{2} a_r V_{LL} \cos \alpha_r - \frac{3\omega L_s}{\pi} I_d \right)$$

$$509.6 \times 10^3 \text{ V} = 2 \times \left(\frac{3}{\pi} \sqrt{2} \times 0.866 \times 230 \times 10^3 \text{ V} \cos \alpha_r - \frac{3 \times 2 \times \pi \times 50 \text{ Hz} \times 1 \times 10^{-3} \text{ H}}{\pi} \times 1200 \text{ A} \right)$$

which gives a rectifier delay angle of $\alpha_r = 18.5^\circ$.

- The maximum link voltage from the 50Hz rectifier, accounting for leakage at maximum current is

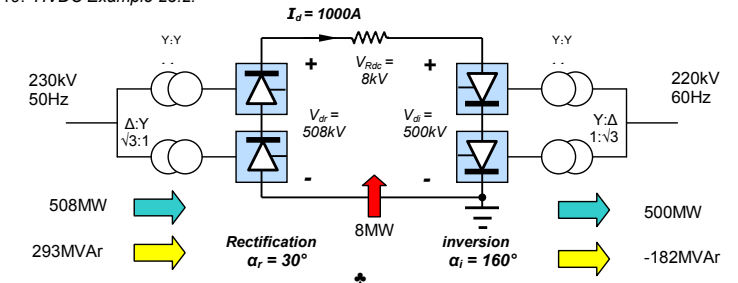
$$V_{dr} = 2 \times \left(\frac{3}{\pi} \sqrt{2} V_{LL} \cos \alpha_r - \frac{3\omega L_s}{\pi} I_d \right)$$

$$\begin{aligned} &= 2 \times \left(\frac{3}{\pi} \sqrt{2} 230 \text{ kV} \times \cos 0^\circ - \frac{3 \times 2 \times \pi \times 50 \text{ Hz} \times 1 \times 10^{-3} \text{ H}}{\pi} 1200 \text{ A} \right) \\ &= 620.5 \text{ kV} \end{aligned}$$

The magnitude of the 600Hz component ($12 \times 50\text{Hz}$) is 15% of 620.5kV, namely 93.1kV, which produces a ripple current of 10% of rated current, 1200A, namely 120A. Thus from $v = L di/dt$

$$\begin{aligned} L_{dc} &= V_{12} \frac{\Delta t_{12}}{\Delta I_{12}} \\ &= 93.1 \text{ kV} \times \frac{1}{12 \times 50 \text{ Hz} \times 120 \text{ A}} = 1.3 \text{ H} \end{aligned}$$

Figure 23.19. HVDC Example 23.2.

**23.8 VSC-based HVDC**

Voltage source converters (VSC) for dc-transmission are one of two-level, neutral point clamped or modular multi-level converters.

Voltage source converter-based (VSC) dc-transmission consists of a bipolar two-wire HVDC system with self-commutable converters connected pole-to-pole, as shown in figure 23.20. DC capacitors are used at each VSC dc-side to provide a stiff dc voltage source. The dc capacitors are grounded at their

electrical centre point to establish the earth reference potential for filtering and the transmission system. The VSC is effectively mid-point grounded and dc filters and a zero-sequence blocking inductor are used to mitigate interference on any metallic communication circuits adjacent to the dc cables. There is no earth return operation. The converters are coupled to the ac system through ac phase inductors and power transformers, with harmonic filters located between the phase inductor and the transformer. The ac filters are tuned to multiples of the switching frequency, as shown in figure 23.24. This arrangement minimizes harmonic currents and avoids dc voltage stresses in the transformer, which allows use of a standard ac power transformer for matching the 50/60Hz AC network voltage to the converter ac voltage necessary to produce the desired dc transmission voltage.

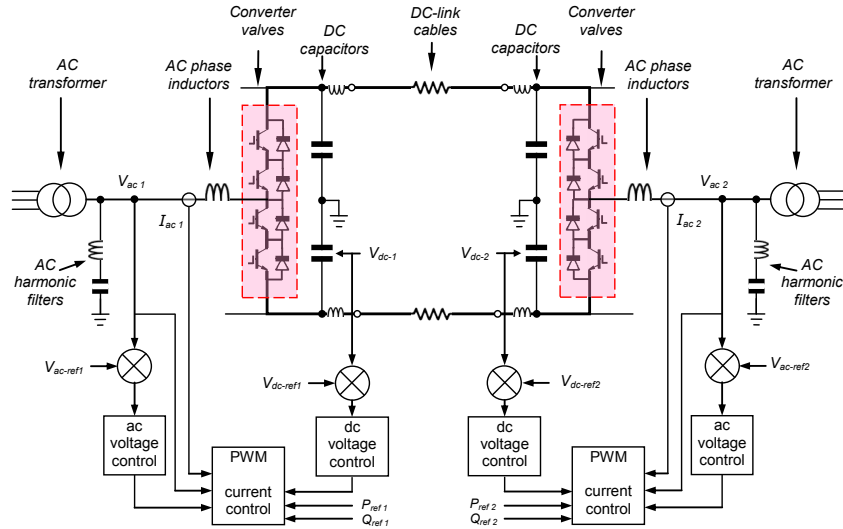


Figure 23.20. Two level symmetrical mono-polar VSC HVDC transmission.

The IGBT valves used in VSC converters are comprised of series-connected IGBT cells. Present technology uses 2.5kV IGBT die, with a 4.5kV objectives, parallel connected on a common electrically-conducting substrate in 2500A sub-modules, with 30 series connected sub-modules in a string cell. Strings are then series connected to produce the required link valve voltage requirement. The IGBT switching frequency is limited to about 2 kHz. The valves are cooled with circulating water and water to air heat exchangers.

The structure is constructed to shield electromagnetic interference (EMI) radiation.

23.8.1 VSC-Based HVDC control

Power flow between the VSC and ac network can be controlled by changing the phase angle of the converter ac voltage V_S with respect to the filter bus ac voltage V_T , whereas the reactive power can be controlled by changing the magnitude of the fundamental component of the converter ac voltage V_T with respect to the filter bus ac voltage V_S . By independently controlling these two aspects of the converter voltage, operation in all four quadrants is possible. This means that the converter can be operated in the middle of its reactive power range near unity power factor to maintain dynamic reactive power reserve for contingency voltage support similar to a static VAR compensator. This also means that the real power transfer can be changed rapidly without altering the reactive power exchange with the ac network or waiting for switching of shunt compensation.

Reactive power control can be used for dynamic voltage regulation to support the ac interconnection, by synthesising a balanced set of three phase voltages. Black start (restoring system operation without an external energy source) capability is also a feature.

Independent control of the VSC ac voltage magnitude and phase relative to the system voltage decouples the active and reactive power control loops for HVDC system regulation. The active power control loop can be set to control either the active power (dc-link current) or the dc-side voltage. In a dc link, one station is selected to control the active power while the other controls the dc-side voltage. The reactive power control loop controls either the reactive power or the ac-side voltage. Either of these two

modes can be selected independently at either end of the dc link. Figure 23.20 shows the characteristic ac voltage phasors including the controlled variables V_{dc} , I_{dc} , Q , and V_L .

23.8.2 Power control concept

dc-link power

The dc-link power flow concepts are not complicated by ac phasor considerations. No reactive power is involved with dc, only the real power flows. Consider the HVDC configuration depicted in figure 23.21 involving converter #1 and converter #2.

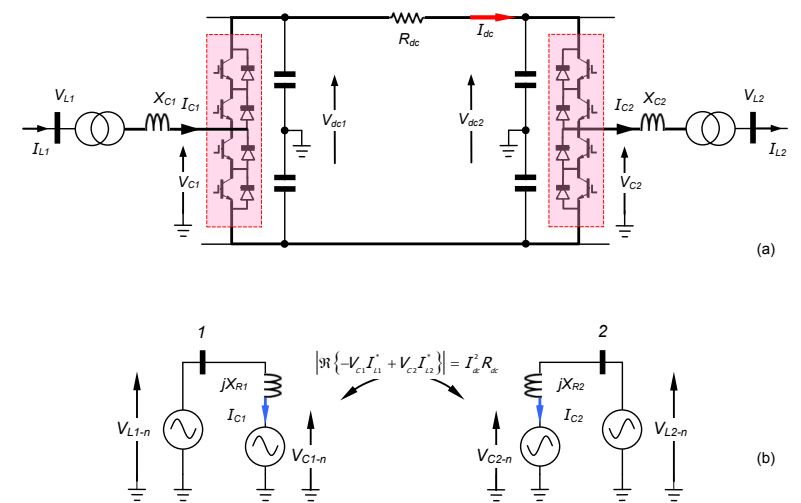


Figure 23.21. VSC HVDC transmission dc-side, using two-level voltage source inverters.

If converter #1 produces an ac voltage represented by

$$\begin{aligned} V_{c1} &= |V_{c1}|(\cos \delta_1 + j \sin \delta_1) \\ &= |V_{c1}| \angle \delta_1 \end{aligned} \quad (23.29)$$

while the other, converter #2, is represented by the voltage source

$$\begin{aligned} V_{c2} &= |V_{c2}|(\cos \delta_2 + j \sin \delta_2) \\ &= |V_{c2}| \angle \delta_2 \end{aligned} \quad (23.30)$$

Then if the power transmitted equals the power received, then

$$\Re\{-V_{c1} I_{L1}^* + V_{c2} I_{L2}^*\} = 0 \quad (23.31)$$

If the dc link resistive losses are incorporated equations (23.31) becomes

$$\Re\{-V_{c1} I_{L1}^* + V_{c2} I_{L2}^*\} = I_{dc}^2 R_{dc} \quad (23.32)$$

ac-side powers

The fundamental base apparent power S_T at the filter bus between the converter reactor and the AC filter is defined as follows (see figure 23.22):

$$S_T = P_T + jQ_T = \sqrt{3} \times V_T \times I_T \quad (23.33)$$

The active and reactive power components on the grid-side are defined as (see section 25.3 of ac power transmission):

$$\begin{aligned} P &= \frac{V_T \times V_S \times \sin \delta}{\omega L} = \frac{V_T \times V_S \times \sin \delta}{X_L} \\ Q_T &= \frac{V_T \times V_S \times \cos \delta - V_T^2}{X_L} \end{aligned} \quad (23.34)$$

where: δ = phase angle between the filtered voltage V_T and the converter output voltage V_S
 L = inductance of the converter ac line inductance

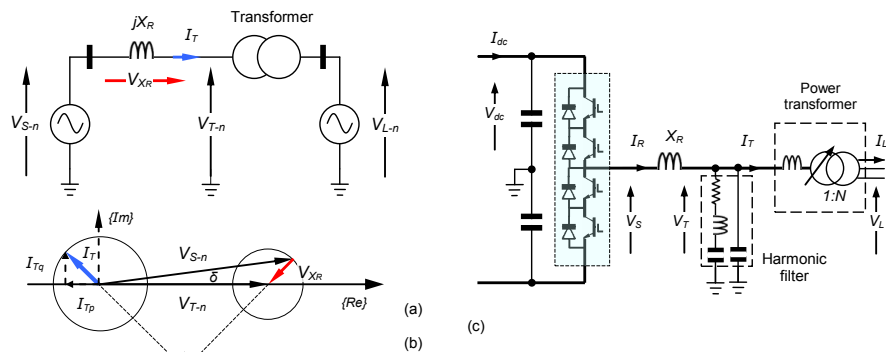


Figure 23.22. VSC HVDC transmission ac-side.

Changing the phase angle δ controls the active power flow P between the converter and the filter bus and consequently the converter and the ac network. The apparent power is $S=P+jQ_T$.

As shown in figure 23.23a, for active power flows:

- if the V_S phase-lags V_T , active power P flows from the ac to the dc side (rectifier)
- if the V_S phase-leads V_T , the active power P flows from the dc to the ac side (inverter)

Changing the amplitude difference between the filter voltage V_T , and the converter voltage V_S controls the reactive power flow between the converter and the ac network.

As shown in figure 23.23b, for reactive power flows:

- if $V_T > V_S$, there is reactive power consumed from the ac network
- if $V_S > V_T$, there is reactive power generated into the ac network

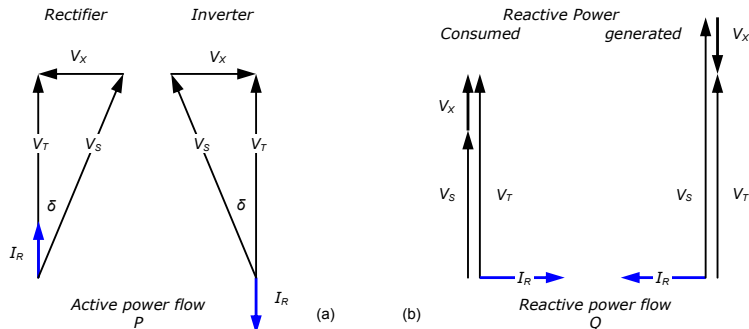


Figure 23.23. Active and reactive power phasor diagrams.

With the PWM (Pulse-Width-Modulation, see Section 17.2.3) controlled VSC it is possible to create any phase angle and voltage amplitude (within limits set by the dc-link voltage magnitude) by changing the PWM modulation depth and the relative phase displacement respectively, by using phase-locked-loop grid synchronised displacement. This allows independent control of the active and reactive power.

The typical P - Q diagram (which depends on the ac system voltage), which is valid within the whole steady-state ac network voltage, is shown in the figure 23.24. This figure illustrates the grid real power, P , and reactive power, Q , capability of the HVDC VSC converter terminal, measured at the interconnection point (point of common coupling, PCC), as a function of ac system voltage. Normally converters are sized based on the specific P - Q envelope, Q - V envelope, and dc link voltage.

The 1st and 2nd quadrants represent rectification and the 3rd and 4th inversion. A positive Q indicates delivery of reactive power to the ac network. Because the dc-link decouples the two converters, reactive power can be controlled independently at each station. There are dc-link voltage (Q generation restrictions) and current (inverter - igbt - power) limitations that have been taken into account in this typical P - Q diagram. Depending on the cable design, the cable dc current maximum may restrict the rectifier power limit. There is also a steady state minimum dc-voltage level limit, which may prevent continuous absorption of large amounts of reactive power.

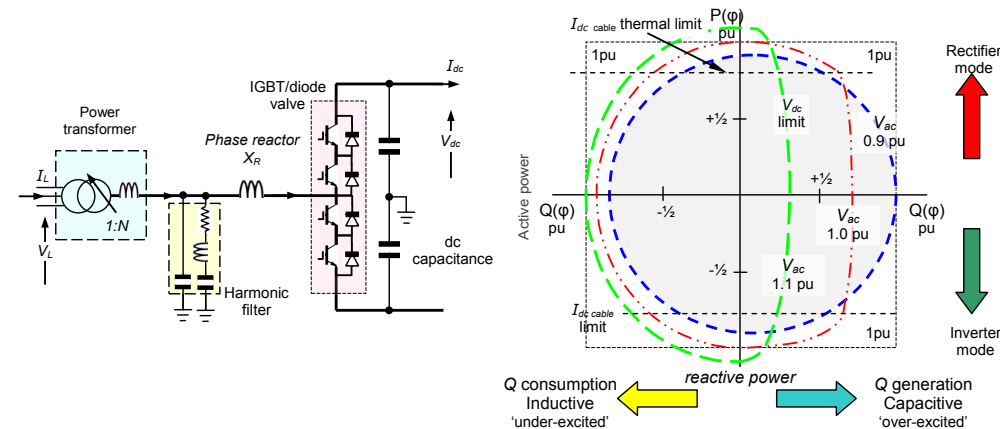


Figure 23.24. P - Q active and reactive power control locus, showing varying voltage limits.

The capacitive reactive power capability increases with decreasing voltage when it is needed most. Similarly, the inductive reactive power capability increases with increasing network voltage when it is needed most. For a given ac system voltage the converter can be operated at any point within its respective 'circle'. At low ac voltages the VA limit dominates. For high ac voltages, the dc-voltage limit is restrictive but it is not desirable to inject reactive power when ac voltage already is high.

23.9 HVDC components

The basic structure of VSC based HVDC system is shown in Figure 23.25. The function and design of the major power components in this and an LCC system follows.

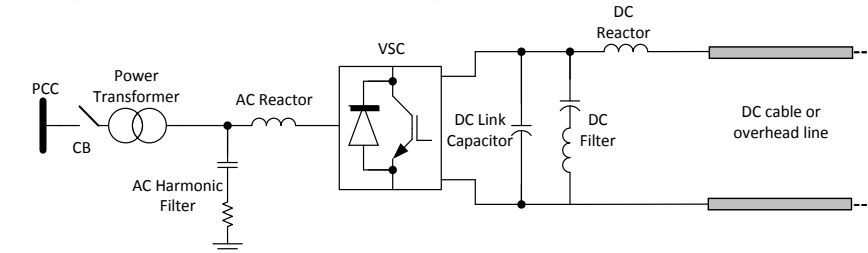


Figure 23.25. Symmetrical mono-polar two-level VSC-HVDC transmission system.

ii. AC Circuit Breaker, CB

AC circuit breakers are used to connect and disconnect the HVDC system during normal and fault conditions. During a dc fault, the ac circuit breaker disconnects the circuit to eliminate feeding the fault from the ac side. There is no special design or requirements compared to normal ac circuit breakers used in power systems. Unlike LCC HVDC, a VSC-based system has no inherent capability to clear dc line faults. A pole-to-pole or pole-to-ground fault will cause the VSC dc capacitor to be discharged and fault current will be maintained via the VSC free-wheeling diodes until the VSC substation ac circuit breakers trip. With a temporary fault, power transmission continues after a normal start-up of the scheme. This can be achieved in the order of 10 seconds.

ii. AC-filters

Two basic shunting filter characteristics are applicable to HVDC, namely high Q tuned filters (band pass) for filtering (shunting) of a specific harmonic and low Q damping filters (high pass) for attenuation (shunting) of more than one high order harmonic.

In a typical HVDC scheme, ac filters contain two or three grounded and/or ungrounded tuned filter branches. A typical second order filter and its frequency characteristics are shown in figure 23.26. AC filters for VSC HVDC converters have lower ratings than those for conventional HVDC converters and are not required for reactive power compensation. These filters are permanently connected to the converter bus and not switched with transmission loading, as in conventional HVDC.

Voltage source converters can be operated with different control schemes, most of which use pulse width modulation to control the ratios (magnitude and phase) between dc and ac side fundamental frequency voltages. At the ac side converter terminal, the voltage to ground is not sinusoidal. The most frequent application of voltage source converters is as a machine drive (in industrial applications) where this is of less concern. However, connecting a voltage source converter to a transmission or distribution system requires the voltage to be sinusoidal. This necessary filtering is achieved by means of the converter inductor and ac filters.

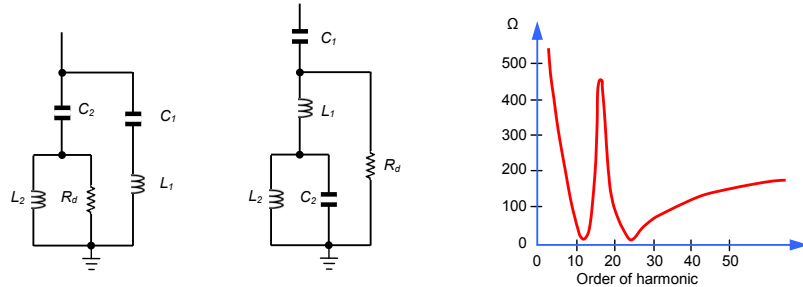


Figure 23.26. Single phase equivalent circuit diagram and harmonic impedance characteristic of a double tuned filter.

The distorted waveform of the converter terminal voltage can be described as a series of harmonic voltages

$$V_s = \sum_{h=1} V_h \cos(h\omega_s t + \alpha_h)$$

where V_h is the h^{th} harmonic voltage.

The magnitude of the harmonic voltages vary with the dc voltage, the switching frequency (or pulse number) of the converter and converter PWM technique. Harmonic cancellation PWM or optimal PWM utilizes a sinusoidal PWM with 3rd harmonic (triplen) injection. A 3rd harmonic is added to the fundamental frequency to increase the voltage, hence power rating of the converter, as considered in chapter 17.1.3.vii.

iii. Converter line inductors

There is one converter oil filled inductor per phase, with EMC shields to eliminate magnetic fields outside the windings. The converter line inductor is a key components in a voltage source converter with which continuous and independent control of active and reactive power is possible.

The main purposes of the converter ac inductors are:

- to provide low-pass filtering of the PWM voltage to give the desired fundamental frequency voltage. The converter generates harmonics related to the switching frequency. The harmonic currents are blocked by the converter inductor and the harmonic content on the ac bus voltage is reduced by an ac shunt filter, which diverts the harmonic currents;
- to provide active and reactive power control. The fundamental frequency voltage across the inductor defines the power flow (both active and reactive) between the ac and dc sides. The P-Q diagram in figure 23.23 shows the active and reactive power definitions;
- to limit line short-circuit currents. The short-circuit voltage of the converter inductor is typically 15%;
- to prevent dc circuit resonance; and
- minimises intermittent dc-link current flow.

The stray capacitance across the line inductor is minimised in order to minimize the harmonics coupled into the ac filter side of the inductor. The high dv/dt on the bridge terminals at switching results in current pulses ($i=C dv/dt$) through all stray capacitances to ground. As these currents pass through the valve,

and should be minimized. The ac filter side of the inductor is effectively at ground at high frequencies and the capacitance across the inductor should therefore be low. To achieve low capacitance the converter inductors have air coils (with a magnetic return circuit) rather than magnetic cores.

iv. Power transformer

Because of the use of the converter ac inductors and the use of VSC PWM, the current in the transformer windings contains minimal harmonics and is not exposed to any dc voltage. The transformer is a number of configured 50/60Hz, two-winding limb, single transformers (because of transportation limitations (size and weight) and redundancy) or a three phase power transformer, with taps and a tap-changer. The secondary voltage, the filter bus voltage, is controlled by the tap changer to achieve the maximum active and reactive power from the VSC, both consumed and generated. The tap changer is located on the secondary side, which has the largest voltage swing, and also to ensure that the ratio between the outer radial line winding and a possible tertiary winding is fixed. This tertiary winding feeds the station auxiliary power system and if delta connected suppresses any core triplen fluxes.

In order to maximize the active power transfer, the converter generates a low frequency zero-sequence voltage ($<0.2pu$) which is blocked by the ungrounded transformer secondary winding.

The power transformer provides the following features:

- Reactance is located between the VSC and the ac system, which decreases the ac filter size.
- Match the voltage between the ac system and the VSC AC terminals, resulting in optimum switch rating utilization.
- Eliminate the 5th and 7th harmonics by connecting the transformer in 12-pulse Yyd configuration.
- Prevents zero sequence current flow between the ac system and the VSC.

Transformer should sustain:

- The fundamental current stresses
- Saturation characteristics of the transformer magnetic field
- Low and middle frequency harmonics stresses
- Dielectric stresses due to normal/transient operating voltage, especially with VSC PWM, and harmonics. The extending composite value-side bushing is tested to higher dc stress levels.

v. DC-link Capacitors

The dc capacitor is the stored energy element for a VSC, providing it with a stiff dc voltage which is essential presumption with VSC topologies. The primary functions of the dc link side capacitor are:

- Provide a low-inductance path for switch turn-off current. Due to the stray inductance, the turn-off commutating current results in transient voltage stresses on the switching devices. These stresses are minimised by reducing connection lengths between the dc link capacitor and the switching devices.
- Temporary energy store, as it stabilises connection operation and facilitates closed loop control adjustment.
- Reduce harmonic dc link voltage ripple. HVDC capacitors use a dry, self-healing, metallised film design, which have advantages over oil filled technologies. A dry capacitor design offers long life, high capacity, and low inductance, in a non-corrosion, non-radiating plastic housing.
- Decreases harmonic coupling between different VSC substations connected to the same dc link.

The dc link capacitor design parameters are:

- Continuous dc operation voltage;
- Limits of dc voltage ripple under transient conditions, such as ac system faults;
- Harmonic currents conducted to the dc side; and
- Peak discharge current during dc faults.

A small voltage ripple requirement implies large capacitance: while small capacitance offers fast active power control. DC capacitor sizing is a trade-off between voltage ripple, lifetime, and fast dc link control. Thus dc link capacitor design bounds is a function of two inequalities:

$$\frac{2\tau S}{V_{dc}^2} > C_{dc} > \frac{S}{2\omega V_{dc} \Delta V_{dc}}$$

where C_{DC} dc-link capacitance, S apparent converter power, V_{DC} rated dc-link voltage, ω electrical frequency, ΔV_{DC} allowed voltage ripple (peak-peak), and τ is the time constant of dc capacitor charging. The time constant τ is selected to be less than 10 ms to satisfy low dc-link voltage ripple.

vi. DC-filters

Instead of over-sizing the dc link capacitor, a series LC filter can be used across the link capacitor to eliminate dangerous harmonics. It is parallel connected to the dc link capacitor to decrease the total equivalent impedance of the dc circuit. This reduces harmonic currents injected into the dc line.

vii. DC-series reactor

In VSC-HVDC systems, a dc reactor (air-core coils with magnetic return paths of iron-core coils with air slots) may be connected after the dc capacitor to:

- Reduce the dc fault current gradient in order to protect VSC free wheeling diodes;
- Harmonic current reduction in the dc overhead line or cable; and
- Critical resonance tuning within the dc circuit.

A dc reactor in a VSC-HVDC system is considerably smaller than that used in an LCC HVDC scheme and typically less than 10mH. To limit dc fault current levels, link inductances approaching those found in LCC HVDC systems tend to be specified.

viii. Overhead and subsea/underground HVDC cables

To transmit electric energy using direct current over a distance, both cables and overhead transmission lines can be used. There is also a small difference between underground and submarine dc cables. The cost of cables is considerably larger than overhead lines but there are also other aspects associated with the basic principle of VSC transmission that may influence the choice:

- Cables often have less impact on the environment than overhead transmission lines.
- It is considerably simpler to obtain right of way for new cables.
- Since a VSC produces only one dc voltage polarity, the cable does not need to be designed for voltage polarity reversal. This allows less expensive and simpler cables, such as extruded XLPE dc cables, to be used in long distance VSC transmission systems.
- Cables are less prone to faults than overhead transmission lines. Since overhead transmission lines are exposed to lightning strikes and pollution, faults along them are likely. Most line outages are transient, with transmission recommencing once air insulation is restored. Permanent faults on overhead lines are easier to repair. In the event of a cable fault, the outage would be permanent and the repair time may be significant.
- VSC HVDC has difficulties coping with dc faults and most existing links operate with dc cables. Manufacturers have been reluctant to offer VSC HVDC with overhead lines, and the 2010 Caprivi VSC HVDC link is the only such installation.

The choice between cables and overhead lines is influenced by environmental constraints as well as an overall optimization that considers total capital cost and transmission system reliability.

DC cable types

HVDC cables are constructed as follows:

- **Conductor**
The shape of the conductor is round and built up of compacted stranded round (copper or aluminium) wires or, for large cross-sections, concentric layers of keystone shaped wires.
- **Insulation system**
The HVDC polymeric insulation system consists of:
 - Conductor screen
 - Insulation
 - Insulation screen
 the insulation system is triple-extruded and dry-cured. (thickness is operating voltage dependant).
- **Metallic screen**
Copper wire screen, for land cables, with cross-section design for fault currents.
- **Metallic sheath**
A lead alloy sheath is provided for submarine cables, while a metal-polyethylene laminate may be provided for land cables. The laminate is bonded to the polyethylene, which gives mechanical properties.
- **Inner jacket (for submarine cables)**
A polyethylene sheath is extruded over the lead sheath to provide mechanical and corrosion protection for the lead sheath.
- **Tensile armour (for submarine cables)**
The tensile armour consists of galvanized round steel wires close to each other helically twisted round the cable, which is flooded with bitumen for corrosion protection. The tensile armour is needed when the cable is laid in the sea. The tensile armour also offers mechanical protection against impacts and abrasion for a cable that is sufficiently buried in the seabed.
- **Outer sheath**
The outer serving for submarine cables consists of two layers of polypropylene yarn, the inner one impregnated with bitumen. The polypropylene yarn is a semi-wet covering.

The outer sheath on land cables is normally a thermoplastic polyethylene (PE) sheath or an extruded halogen PVC flame-retardant sheath. PE is a harder material offering better mechanical protection.

For long term physical cable integrity, the surface of the outer sheath may be provided with a thin conductive layer, which is simultaneously extruded with, and thus strongly bonded to, the non-conductive underlying jacket.

Additionally optic fibre cable for communication purposes, may be laid with the bundled.

The most common cable technologies include:

- Mass-impregnated (MI) insulation cables
- Low-pressure oil-filled (LPOF) cables
- Extruded cross-linked polyethylene (XLPE) cables

a) Mass-impregnated single core mass cables

MI insulation is made by winding kraft processed paper around the conductor until the required insulation thickness is achieved. The cable is then placed in a vacuum chamber and heated to remove any air and moisture. A viscous oil is introduced which impregnates the paper, increasing the electrical strength of the insulation. A recent development uses polypropylene laminated papers, where thin layers of plastic are laminated to the paper layers, allowing the cable to operate at higher temperatures and therefore higher current ratings. HVDC,

For bulk power transmission, mass impregnated cables prove to be the most suitable solution because of their capacity to operate up to ± 600 kV dc (1600A , 2500mm^2) and transmission capacity over 1000 MW for monopole solutions. Therefore an HVDC in bipolar connection is able to transmit up to 2GW with MI cables. These cables can be installed at depths to 1000m under the sea level and with nearly unlimited transmission length. The system capacity is limited by the conductor temperature, which can reduce overload capability. Most submarine cables are the mass-impregnated type. Figure 23.27a shows a photo of mass impregnated cable manufactured by ABB.

Also these cables tolerate fast dc voltage polarity reversal making them suitable for LCC HVDC.

b) Low pressure oil filled (LPOF) cables

LPOF cables are insulated with paper impregnated with low viscosity oil under an overpressure of a few bars. This ensures voltages up to 500 kV and capabilities up to 1000 MW for underground installations. It can be used for both ac and dc transmission applications. Since oil flow is required along the cable, the cable length is limited to around 80 km. Environmentally, the risk of oil leakage must be taken into account.

c) Extruded Cross linked polyethylene (XLPE) cables

XLPE cables offer a high working temperature, and use a lapped non-impregnated thin polyethylene film insulator extruded over the cable core, to allow long and deep submarine installation, associated with increased electrical operational stresses. A bonded metal-polyethylene laminate can be bonded can help ensure cable physical integrity.

XLPE cables are available up to $\pm 320\text{kV}$ dc, giving 1000MW per bipolar, with development aimed at increasing the voltage rating of cable technology and reducing its cost. This will make VSC transmission more attractive for a number of applications. Most underground cable insulators are made from extruded insulation. Figure 23.27b shows a XLPE cable. XLPE cables are unsuitable for use in CSC applications where, in order to reverse the direction of power flow, the polarity must be reversed.

Underground and submarine cables

Three types of cables are used for underground and submarine cables as shown in Table 23.1. The different between the underground and submarine cables are the conductor material and the armour layer, which is used in submarine cables to withstand the axial mechanical tension during laying and operation.

Cables with copper conductors are used for submarine applications and aluminium conductors for land. Cable ratings for bipolar VSC-HVDC are double those shown in table 23.1. Cu has high electrical conductivity and mechanical properties; being easy to create strong joints. However it is heavy and more expensive, thus is used when its mechanical properties are mandatory, such as submarine cables. Al has low conductivity and low mechanical properties; being difficult to implement joints. It is lighter and cheaper than Cu.

Table 23.1. Cables for underground and submarine application

Type		Mass-impregnated	LPOF	XLPE
Conductor		Cu/Al	Cu/Al	Cu/Al
Insulation		Paper and mass	Paper and fluid	Cross linked PE
Voltage	kV	600	500	320
Maximum conductor size	mm ²	3000	3000	2400
Maximum current	A	2000	2000	2700
Capacity per Cable	MW	1000	600	1000
Weight	kg/m	30-60	40-80	15-61
Converter type		LCC or VSC	LCC or VSC	VSC or unidirectional LCC

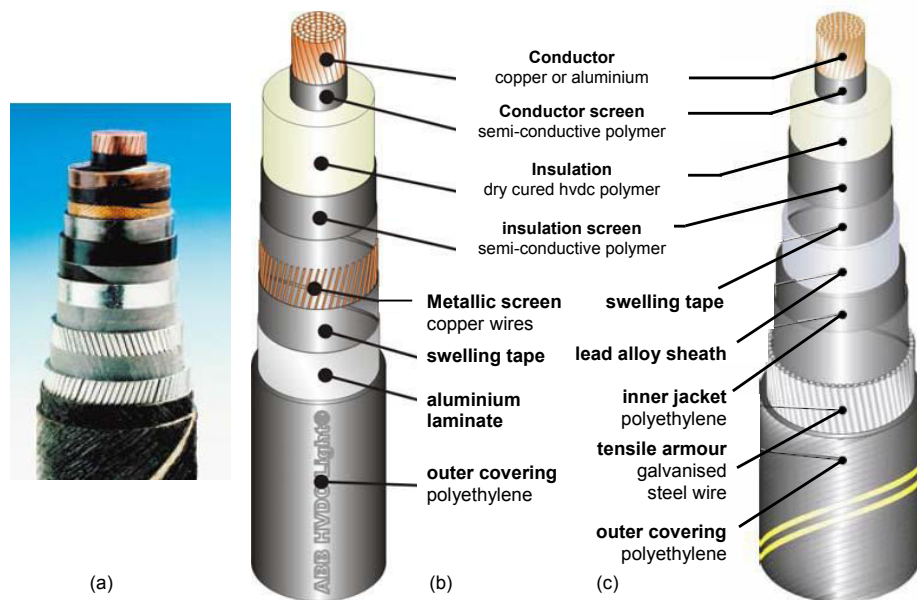


Figure 12.27. ABB HVDC cables: (a) mass impregnated, MI, (b) XLPE land and (c) XLPE submarine.

DC cable modelling

In basic low frequency dynamic studies, dc cables are represented as lumped T or π models as shown in Figure 23.28. The cable parameters are a function of the cable length. For example, the parameters of a 500 kV, 2000 A dc cable are: R=0.05 Ω/km, C= 0.26 μF/km.

In more detailed studies, for example, mid cable dc faults, a distributed parameter model is used.

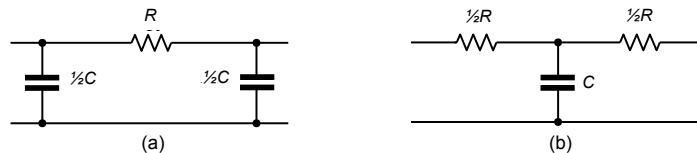


Figure 23.28. Basic cable: (a) T model and (b) π model.

DC cable environmental factors

Electro Magnetic Fields (EMF)

DC power transmission, via underground cable, generates low frequency magnetic fields in the range of 50μT, which is the same order as the background static magnetic field of the earth, which are 8,000 times lower than the 400mT deemed the accepted threshold assessed as no risk to human health.

Magnetic field

HVDC cables are laid in pairs, close together, carrying the same current levels in opposite directions, so the overlapping static magnetic fields tend to cancel each other out. The resulting magnetic field decreases rapidly to zero with distance from the cables.

Acoustic noise

Unlike ac transmission lines, HVDC cables do not make noise, unlike all converter stations.

Ground heating

During operation, the temperature of an underground cable will rise dependent on the current carried and load factor. Heat distribution to surrounding soil depends on the backfill material. The impact of heat release on soil temperature is strictly local and very limited. Typically 1°C above the line at 1m depth.

ix. HVDC dc circuit breaker

High-current high-voltage dc circuit breakers are problematic. Semiconductor approaches involve series connection of many devices, resulting voltage sharing problems and high on-state losses. Hybrid approaches use a combination of semiconductors for turn-off speed and vacuum circuit breakers for low losses. The utilisation of dc circuit breakers is problematic in a multi-terminal hvdc system since clearing and isolation are required both sides of the dc fault. Polymer or porcelain housed metal oxide (ZnO) surge arresters are vital in all hvdc systems, and are extensively used in all dc circuit breakers.

Example 23.3: HVDC transmission with voltage source controlled dc-link #1

A 200kV, 1000A, HVDC is being considered as interconnection between two ac systems as shown in Figure 23.29. As shown the HVDC converter ratings are 200MVA. The 50Hz load inverter grid draws a total of 150MVA at a 0.75 power factor, while the rectifier VSC draws the power requirement from the 60Hz network at unit power factor. Sinusoidal Pulse Width Modulation (SPWM) is used with triangular carrier wave with a frequency 1350 Hz. The copper dc cable is 1000 mm², with total distance 100 km. Assuming copper has specific resistance of R=1.39×10⁻² Ω /km, determine:

- Transformer turns ratio for the rectifier and inverter transformers.
- DC cable losses.
- Active and reactive power delivered at the inverter side.
- Active and reactive power drawn at the rectifier side.

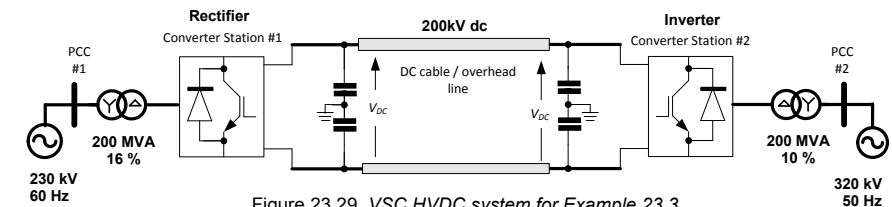


Figure 23.29. VSC HVDC system for Example 23.3.

Solution

- On the inverter side:

$$V_{dc\ 50Hz} = 200kV$$

$$V_{LN\ 50Hz} = \frac{V_{dc\ 50Hz}}{2\sqrt{2}} = 70.721kV$$

$$V_{LN\ 50Hz-at-star-side} = \sqrt{3}V_{LN\ 50Hz} = 122.347kV$$

$$L_{tr} = X_{tr} \frac{V_{pr}^2}{S_t} = 0.10 \frac{320\text{kV}^2}{200\text{MVA}} = 51.5\Omega$$

$$I_{L50\text{Hz}} = \frac{S_{50\text{Hz}}}{\sqrt{3} \times V_{L50\text{Hz}}} = \frac{200\text{MVA}}{\sqrt{3} \times 320\text{kV}} = 361.271\text{A}$$

$$V_{L-N \text{ conv}50\text{Hz-est}} = V_{L-N \text{ grid}50\text{Hz}} + jX_L I_L$$

$$= 320/\sqrt{3} + j51.5 \times 361.271 = 185\text{kV} + j18.497\text{kV}$$

$$= 203.497\text{kV}$$

The transformer turns ratio is $203.497\text{kV}/122.347\text{kV} = 1.663$

On the rectifier side:

$$V_{dc60\text{Hz}} = V_{dc50\text{Hz}} + I_{dc} R_{dc} = 200\text{kV} + 1000\text{A} \times 1.39\Omega = 201.39\text{kV}$$

$$V_{LN60\text{Hz}} = \frac{V_{dc60\text{Hz}}}{2\sqrt{2}} = 71.212\text{kV}$$

$$V_{LN60\text{Hz-at-star-side}} = \sqrt{3} V_{LN60\text{Hz}} = 123.198\text{kV}$$

$$L_{tr} = X_{tr} \frac{V_{pr}^2}{S_t} = 0.16\Omega \frac{230\text{kV}^2}{200\text{MVA}} = 42.32\Omega$$

$$I_{L60\text{Hz}} = \frac{S_{60\text{Hz}}}{\sqrt{3} \times V_{L60\text{Hz}}} = \frac{200\text{MVA}}{\sqrt{3} \times 230\text{kV}} = 502.63\text{A}$$

$$V_{L-N \text{ conv}60\text{Hz-est}} = V_{L-N \text{ grid}60\text{Hz}} + jX_L I_L$$

$$= 230\text{kV} / \sqrt{3} - j42.32\Omega \times 502.63\text{A} = 133\text{kV} - j21.271\text{kV} = 111.729\text{kV}$$

The transformer turns ratio is $111.729\text{kV}/123.198\text{kV} = 0.9$

ii. DC cable losses

$$R_{dc} = 2R_{oCu} \ell_{cu} = 2 \times 1.39 \times 10^{-2} \times 100\text{km} = 2.78\Omega$$

$$P_{dc \text{ loss}} = I_{dc}^2 R_{dc} = 1000\text{A}^2 \times 2.78\Omega = 2.78\text{MW} = 1.39\% \text{ of } 200\text{MW}$$

iii. The total active 50Hz power at the inverter is

$$P_{50\text{Hz}} = S_{50\text{Hz}} \times \text{pf}_{50\text{Hz}}$$

$$= 150\text{MVA} \times 0.75 = 112.5\text{MW}$$

The 50Hz reactive power flow into the DC link is

$$Q = \sqrt{VA^2 - P^2}$$

$$= \sqrt{150^2 - 112.5^2} = 99.21\text{MVAr}$$

iv. At rectifier side:

$$P_{rec} = 112.5\text{MW} + 2.78\text{MW} = 115.28\text{MW}$$

$$Q_{rec} = 0$$



Example 23.4: HVDC transmission with voltage source controlled dc-link #2

The VSC dc-voltage transmission line represented by figure 23.26 connects a 130kV ac rms, 50Hz three-phase system to a 120kV, 60Hz three-phase system, some 100km apart. The voltage-controlled converter at each nominal $\pm 80\text{kV}$ transmission line end are interface by a Δ -Y transformer with 25mH of line and leakage reactance referred to the grid side, and with a turns ratio to match the converter voltage requirements for the $\pm 80\text{kV}$ dc link. The cable is rated at 625A with 300mm^2 of copper giving a total line resistance is 2Ω .

The 50Hz load end grid draws a total of 100MVA at a 0.75 power factor, while source end VSC draws the power requirement from the 60Hz network at unit power factor.

Determine the phasor diagram for:

- the 50Hz receiving end
- the 60Hz transmitting end.

Solution

i. The total active 50Hz power at the load end is

$$P_{50\text{Hz}} = S_{50\text{Hz}} \times \text{pf}_{50\text{Hz}}$$

$$= 100\text{MVA} \times 0.75 = 75\text{MW}$$

The 50Hz reactive power flow into the dc link is

$$Q = \sqrt{VA^2 - P^2}$$

$$= \sqrt{100^2 - 75^2} = 66.1\text{MVAr}$$

The 50Hz ac line current is

$$I_{L50\text{Hz}} = \frac{S_{50\text{Hz}}}{\sqrt{3} \times V_{L50\text{Hz}}}$$

$$= \frac{100\text{MVA}}{\sqrt{3} \times 130\text{kV}} = 441\text{A}$$

The necessary phasor diagram is referenced with respect to neutral.

The reference 50Hz phase voltage is

$$V_{L-N50\text{Hz}} = \frac{V_{L50\text{Hz}}}{\sqrt{3}}$$

$$= \frac{130\text{kV}}{\sqrt{3}} = 75.06\text{kV} \angle 0^\circ$$

The angle between the line current and the phase voltage is

$$\theta = \cos^{-1} 0.75 = 41.4^\circ$$

The line reactance at the 50Hz end is

$$X_{L50\text{Hz}} = 2\pi f \times L$$

$$= 2\pi \times 50\text{Hz} \times 25\text{mH} = 7.85\Omega$$

The 50 Hz converter line to neutral voltage (and load angle) is

$$V_{L-N \text{ conv}50\text{Hz}} = V_{L-N50\text{Hz}} + jX_L I_L$$

$$= 75\text{kV} + j7.85\Omega \times 441\text{A} \angle -41.4^\circ$$

$$= 75\text{kV} + 3.45 \angle 48.6^\circ = 77.3\text{kV} + j2.59$$

$$= 77.34\text{kV} \angle 1.92^\circ$$

The line-to-line voltage at the 50Hz VSC converter is

$$V_L = \sqrt{3} V_{L-N}$$

$$= \sqrt{3} \times 77.34\text{kV} = 134\text{kV}$$

ii. The $\pm 80\text{kV}$ dc-link has a pole-to-pole voltage of 160kV. From $P_i = V_{di} \times I_d$, the link current is

$$I_d = \frac{75\text{MW}}{160\text{kV}} = 468.75\text{A}$$

The cable voltage drop is

$$V_{dc} = I_d \times R_{dc}$$

$$= 468.25\text{A} \times 2\Omega = 0.9375\text{kV}$$

The VSC converter dc voltage at the 60Hz transmitting end is $160\text{kV} + 0.938\text{kV} = 160.938\text{kV}$ such the pole voltages are $\pm 80.469\text{kV}$. These results are shown in figure 23.30.

The VSC power delivered into the link is

$$P_{dc60\text{Hz}} = I_d V_{dc60\text{Hz}}$$

$$= 468\text{A} \times 2 \times 80.47\text{kV} = 75.36\text{MW}$$

With unity power at the 60Hz sending end $P = S$, the line current is

$$I_{L60\text{Hz}} = \frac{S_{60\text{Hz}}}{\sqrt{3} V_L} = \frac{P_{60\text{Hz}}}{\sqrt{3} V_L}$$

$$= \frac{75.36\text{MW}}{\sqrt{3} \times 120\text{kV}} = 362.6\text{A}$$

For the 60Hz transmission end phase or diagram, the line to neutral voltage is required from the 120kV line voltage at the 60Hz end, thus

$$V_{L-N\ 60\text{Hz}} = \frac{V_{L60\text{Hz}}}{\sqrt{3}} = \frac{120\text{kV}}{\sqrt{3}} = 69.3\text{kV}$$

The 60Hz line reactance is

$$X_{L60\text{Hz}} = 2\pi f \times L_{60\text{Hz}} = 2\pi \times 60\text{Hz} \times 25\text{mH} = 9.45\Omega$$

The 60Hz VSC converter side-line to neutral voltage is therefore

$$\begin{aligned} V_{L-N\text{conv}\ 60\text{Hz}} &= V_{L-N\ 60\text{Hz}} - jX_{L60\text{Hz}} I_{L60\text{Hz}} \\ &= 69.3\text{kV} - j9.45\Omega \times 362.6\text{A} \angle 0^\circ \\ &= 69.3\text{kV} + 3.426\text{kV} \angle -90^\circ \\ &= 69.385\text{kV} \angle -2.83^\circ \end{aligned}$$

The line voltage at the sending converter is

$$\begin{aligned} V_{L\text{conv}\ 60\text{Hz}} &= \sqrt{3} V_{L-N\text{conv}\ 60\text{Hz}} \\ &= \sqrt{3} \times 69.385\text{kV} = 120.18\text{kV} \end{aligned}$$

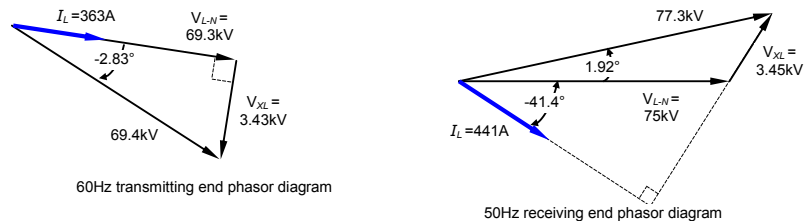
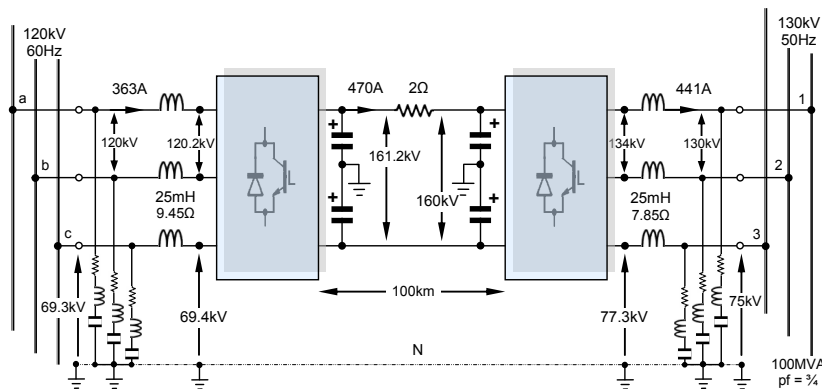
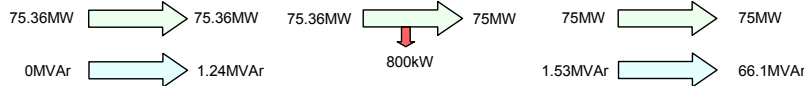


Figure 23.30. HVDC VSC Example 23.4.

Example 23.5: HVDC transmission with voltage source controlled dc-link #3

Figure 23.31 shows one terminal of a 500MW VSC HVDC system. If the converter is rated at $P_{dc} = 500\text{MW}$ and $Q = \pm 100\text{MVAR}$, determine:

- i. the rms current in switches,
- ii. the rms current in switches for a dc fault near dc bus, as indicated. Comment on the result, considering the converter switches.
- iii. Hence the dc fault current in the dc cable for this RMS fault current.

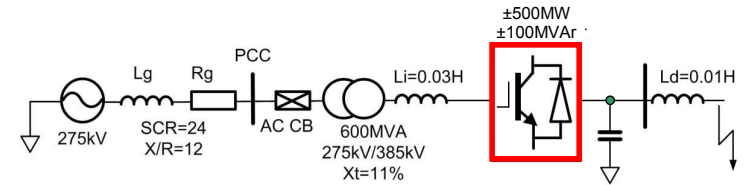


Figure 20.31. VSC HVDC terminal in example 23.5.

Solution

i. The total converter (apparent) power:

$$S_c = \sqrt{P_c^2 + Q_c^2} = \sqrt{(500 \times 10^6)^2 + (100 \times 10^6)^2} = 510\text{MVA}$$

whence the converter current is:

$$\begin{aligned} I_c &= \frac{S_c}{\sqrt{3} V_c} \\ &= \frac{510\text{MVA}}{\sqrt{3} \times 385 \times 10^3} = 765\text{A} \end{aligned}$$

ii. From the SCR expression

$$z_{sm} = \frac{V_s^2}{SCR \times P_{dc}} = \frac{275,000^2}{24 \times 500 \times 10^6} = 6.3\Omega$$

The ac grid resistance is

$$\begin{aligned} R_g &= \frac{z_g}{\sqrt{1 + (X/R)^2}} \\ &= \frac{6.3}{\sqrt{1 + 12^2}} = 0.5234\Omega \end{aligned}$$

and the ac grid reactance is

$$\begin{aligned} X_g &= R_g \times X/R \\ &= 0.5234\Omega \times 12 = 6.28\Omega \end{aligned}$$

Hence the ac grid impedance, referred to grid side, is:

$$\begin{aligned} z_s &= R_g + (X_g + X_t) + jX_l / n_t^2 \\ &= 0.5234\Omega + (6.28\Omega + 0.11 \frac{275\text{kV}^2}{600\text{MVA}}) + j2\pi 50 \times 0.03 \times (275\text{kV}/385\text{kV})^2 \\ &= 6.302\Omega \end{aligned}$$

Note that the dc side inductor has no impact on the fault current.

Converter ac fault current is:

$$\begin{aligned} I_{ac\ \text{fault}} &= \frac{V_g / \sqrt{3}}{z_s} \times (275\text{kV}/385\text{kV}) \\ &= \frac{275\text{kV} / \sqrt{3}}{6.302\Omega} \times (275\text{kV}/385\text{kV}) = 4544\text{A} \end{aligned}$$

This fault current is almost 6 times the rated current, 765A. Typical IGBT reverse diodes would take this current for less than 20ms. This might be too short time for ac CB to clear the fault. In this HVDC system the phase reactors L_l would need to be increased, if possible.

iii. The dc fault current is:

$$\begin{aligned} I_{dc\ \text{fault}} &= \frac{\pi}{\sqrt{6}} I_{ac\ \text{fault}} \\ &= \frac{\pi}{\sqrt{6}} 4544\text{A} = 5828\text{A} \end{aligned}$$

Example 23.6: HVDC transmission with voltage source controlled dc-link #4

Consider the same VSC HVDC terminal as in the previous example (figure 23.31), assuming the PCC bus voltage is controlled to 275kV.

Determine:

- i. the converter AC voltage for maximum power demand
 - a) $P_c=+500\text{MW}$, $Q_c=+100\text{MVar}$
 - b) $P_c=-500\text{MW}$, $Q_c=-100\text{MVar}$

Refer the converter voltage to grid side and determine the percentage voltage swing.

- ii. the maximum ac voltage swing, assuming the phase reactance is increased 4 times to contain dc faults.

Solution

Assuming the reference coordinate frame is linked to the PCC voltage, then the converter current is:

$$I_c = \frac{1}{\sqrt{3}} \frac{V_{ac} - V_c}{j(X_t + X_l)} = \frac{1}{\sqrt{3}} \frac{V_{ac} - V_{cx} - jV_{cy}}{j(X_t + X_l)}$$

$$I_{cx} + jI_{cy} = \frac{1}{\sqrt{3}} \frac{-V_{cy}}{X_t + X_l} - j \frac{1}{\sqrt{3}} \frac{V_{ac} - V_{cx}}{X_t + X_l}$$

The PCC power is:

$$P_c - jQ_c = \sqrt{3}V_{ac}I_{cx} + j\sqrt{3}V_{ac}I_{cy}$$

$$= \frac{-V_{ac}V_{cy}}{X_t + X_l} - jV_{ac} \frac{V_{ac} - V_{cx}}{X_t + X_l}$$

Therefore the voltage components are

$$V_{cd} = -\frac{Q_{ac}(X_t + X_l)}{V_{ac}} + V_{ac}$$

$$V_{cq} = -\frac{P_{ac}(X_t + X_l)}{V_{ac}}$$

i. a)

$$V_{cd} = -\frac{Q_{ac}(X_t + X_l)}{V_{ac}} + V_{ac}$$

$$= -\frac{100\text{MVar} \left(0.11 \frac{275\text{kV}^2}{600\text{MVA}} + 2\pi \times 50 \times 0.03 \times \left(\frac{275\text{kV}}{385\text{kV}} \right)^2 \right)}{275\text{kV}} + 275\text{kV}$$

$$-12\text{kV} + 275\text{kV} = 263\text{kV}$$

$$V_{cq} = -\frac{P_{ac}(X_t + X_l)}{V_{ac}}$$

$$= -\frac{500\text{MW} \left(0.11 \frac{275\text{kV}^2}{600\text{MVA}} + 2\pi \times 50 \times 0.03 \times \left(\frac{275\text{kV}}{385\text{kV}} \right)^2 \right)}{275\text{kV}}$$

$$= -60\text{kV}$$

$$V_{c \min} = \sqrt{V_{cd}^2 + V_{cq}^2} = \sqrt{60000^2 + 263000^2} = 269.76\text{kV}$$

$$\Delta V_{\min} \% = \frac{V_{ac} - V_{c \min}}{V_{ac}} 100 = \frac{275\text{kV} - 269.76\text{kV}}{275\text{kV}} 100 = 1.7\%$$

i. b) With P_{ac} and Q_{ac} reversed

$$V_{cd} = -\frac{Q_{ac}(X_t + X_l)}{V_{ac}} + V_{ac}$$

$$12\text{kV} + 275\text{kV} = 287\text{kV}$$

$$V_{cq} = -\frac{P_{ac}(X_t + X_l)}{V_{ac}}$$

$$= 60\text{kV}$$

$$V_{c \max} = \sqrt{V_{cd}^2 + V_{cq}^2} = \sqrt{60\text{kV}^2 + 287\text{kV}^2} = 293.3\text{kV}$$

$$\Delta V_{\max} \% = \frac{V_{ac} - V_{c \max}}{V_{ac}} 100 = \frac{275\text{kV} - 293.3\text{kV}}{275\text{kV}} 100 = -3.2\%$$

This voltage swing, $1.7\% - 3.2\% = 4.9\%$, is relatively small.

ii. Repeating the same procedure with $L_l = 0.12\text{H}$:

$$\Delta V_{\min} \% = 1.9\%$$

$$\Delta V_{\max} \% = -6.6\%$$

The total voltage swing is $1.9\% - 6.6\% = 8.5\%$, which is acceptable, but should account for when dimensioning equipment.

**23.10 Twelve-pulse transformer based HVDC**

Figure 23.32 show a HVDC configuration that takes advantage of a star-delta, phase-shifting, transformer secondary to halve the series IGBT connection problems associate with high-voltage applications. The twelve-pulse transformer arrangement also reduces the 5th and 7th ac harmonics due to the cancellation effect because of the 30° phase shift between the two secondary windings. These advantages are traded against the complexity associated with an extra high-voltage transformer winding. A VSC variation is to use multilevel configurations involving chained cells, called a capacitor clamped multilevel M²C converter. The cell comprise is a capacitor of large capacitance, which is switched in and out of the series string circuit, as introduced in chapter 17.3.4 and considered in 23.13.

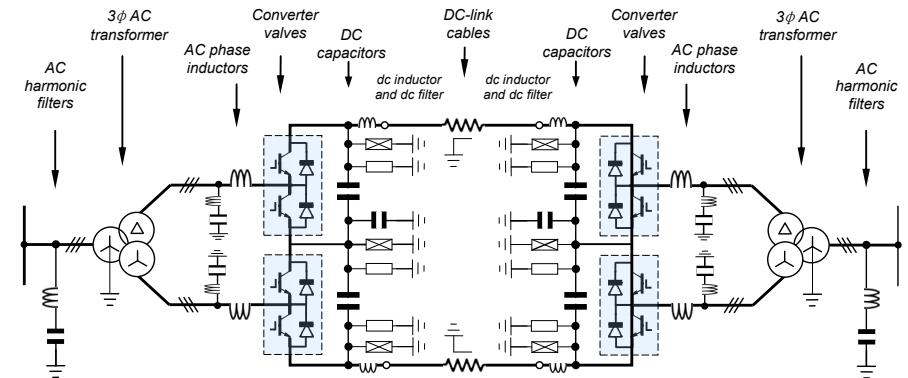


Figure 23.32. HVDC NPC VSC using twelve-pulse transformer arrangement.

23.11 VSC-HVDC transmission systems based on the modular multilevel converter, M²C

The M²C approach exploits the potential of a multilevel structure and pulse width modulation. The filtering requirements are reduced due to generation of high quality ac voltage (small filters are required). The use of a large number of levels with small voltage steps, results in low dv/dt and reduced voltage stress on the insulation of the interfacing transformers. This allows the use of standard 50/60Hz transformers without need to withstand dc link voltage or harmonic currents. The effective switching frequency per device is low, which reduces the switching losses and overall conversion losses, and does not produce significant high frequency noise. Fig. 23.33 shows one-phase of a 7-level modular converter, which relies on the cell capacitors to create a multilevel voltage waveform at the converter terminal. As the number of levels increases, it can generate high voltage with low harmonic content, using medium voltage devices (2.5kV or 4.5kV). DC link capacitors are not required, which significantly reduces the space requirement for the converter station. As the converter depends on phase voltage redundancy to maintain approximately constant voltage across the cell capacitors, the modular multilevel converter performs better than the NPC converter during unbalanced operation, and symmetrical and asymmetrical faults, without increasing the risk of device failure or system collapse. The ability of the modular converter to ride through different types of ac faults makes it attractive in power system applications where restrictive grid codes must be met. The absence of the dc link

capacitors in VSC-HVDC transmission system based on the modular converter, make sizing the cell capacitors critical. They are sized to be able to store enough energy to support the converter dc link during transient events, otherwise the system may fail to meet transient ride-through requirements. The first commercial modular multilevel converter based HVDC transmission system project is the Trans Bay cable project in USA, rated at 400MW active power transfer and $\pm 170\text{MVar}$ STATCOM functionality with a bipolar dc link voltage of $\pm 200\text{kV}$. The line is 85km of submarine cable.

For this type of multi-level converter, the cell capacitors experience the full load current, unlike the rail capacitor of a two level system. High capacitance and large physical size result. This capacitance is the dominant factor in the size of this type of converter. But the main dc link capacitors in both ends of the line are eliminated. There is dc current component in the leg current and no dc link fault protection is offered.

The essential features of the m^2c are

- A highly modular construction both in the power section and in control and protection, allowing a converter hall with a small footprint or a building with a low profile.
- In normal operation, only one level per converter arm switches at any given time. Thus the ac voltages can be adjusted in small increments and a dc voltage with little ripple can be achieved, which minimizes the level of generated harmonics and in most cases eliminates the need for ac filters. Additionally, the small output voltage steps produce minimal radiated or conducted high-frequency interference.
- The low switching frequency of the individual semiconductors results in low switching losses, thus resulting in high system efficiency.
- Uses standard proven components.
- The produced voltages and currents (low di/dt and dv/dt) allow the use of standard ac transformers.
- Fast system response to faults, particularly ac faults.

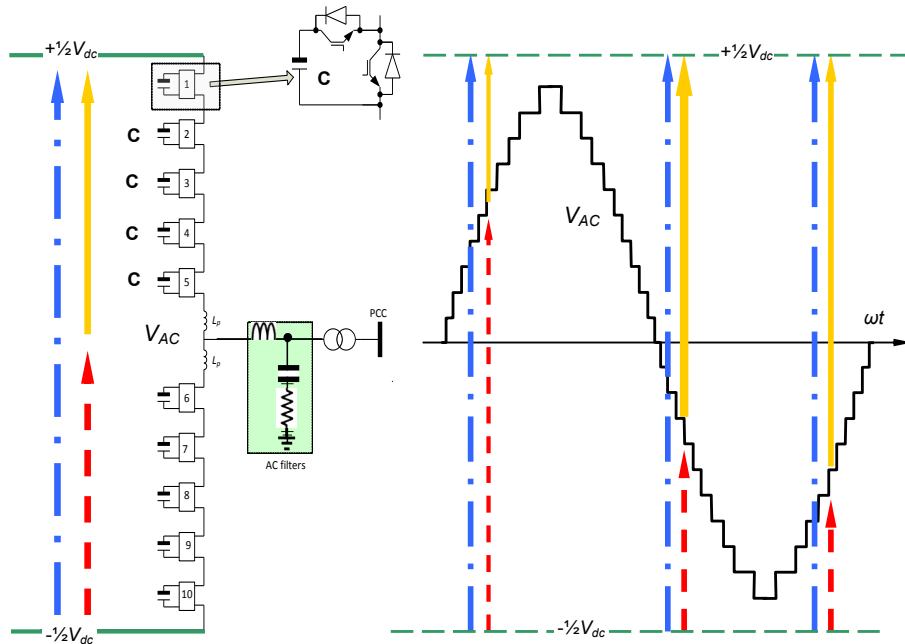


Figure 23.33: One-phase of 7-level modular converter used as basic HVDC building block and components of the ac output voltage before filtering.

Table 23.2: Comparison between different HVDC technologies

	Current source converter based		Voltage source converter based		
	LCC line commutated converter	CCC capacitor commutated converter	Two-level	Neutral-point clamped (3 level)	Modular (M^2C) (half bridge)
Switching device	Thyristor	Thyristor	IGBT	IGBT	IGBT
switching losses	negligible	negligible	high	moderate	low
On-state losses	low	low	moderate	moderate	moderate
Station size	large	Reduced due elimination of switch capacitors and their circuit breakers	Significantly reduced (30% to 50% of LCC)	Significantly reduced (30% to 50% of LCC)	Significantly reduced (30% to 50% of LCC)
Active power control	continuous from $\pm 10\%$ to $\pm 100\%$	continuous from $\pm 10\%$ to $\pm 100\%$	Continuous From 0 to $\pm 100\%$	Continuous From 0 to $\pm 100\%$	Continuous From 0 to $\pm 100\%$
Active power reversal	DC voltage polarity must be changed and not instantaneous (0.5-1s)	DC voltage polarity must be changed and not instantaneous (0.5-1s)	Instantaneous and no change of DC voltage polarity	Instantaneous and no change of DC voltage polarity	Instantaneous and no change of DC voltage polarity
Independent control of active and reactive power	no	no	yes	yes	yes
Reactive power demand	50% to 60%	20% to 50%, with additional series capacitance	no	no	no
Reactive power capability	Limited (lagging VAR only) and discontinuous using switch shunt capacitors for leading VAR	Limited (lagging VAR only)	Continuous and inherent within the converter control at no additional cost	Continuous and inherent within the converter control at no additional cost	Continuous and inherent within the converter control at no additional cost
Power levels	Up to 6400MW	Up to 6400MW	Up to 1200MW	Up to 1200MW	Up to 1200MW
Controllability - Response time	Low (0.1-0.2s)	Low (0.1-0.2s)	High (0.03-0.05s)	High (0.03-0.05s)	High (0.03-0.05s)
AC filters	large	large	small	< 2-level converter	no
DC filter	yes	yes	no	no	no
Converter transformer	Expensive with high insulation requirement to withstand voltage stresses during power reversal	Expensive with high insulation requirement to withstand voltage stresses during power reversal, but with reduced MVA rating	Expensive with high insulation requirement to withstand switching of large voltage steps with high frequency. Additional large AC inductor is needed.	Expensive with high insulation requirement to withstand switching of large voltage steps with high frequency. Additional large AC inductor is needed.	Cheap with standard insulation. Additional large AC inductor is needed.
DC cable	Expensive with high insulation requirement to withstand voltage stresses during power reversal	Expensive with high insulation requirement to withstand voltage stresses during power reversal	Cheap and light weight extruded cable	Cheap and light weight extruded cable	Cheap and light weight extruded cable
Commutation failure	Due to voltage distortion and lack of reactive power during AC fault	Significantly reduced	no	no	no
Applications	Connection of strong systems only (SCR>2.5), connection of weak system is possible but at additional cost by using STATCOM or synchronous condenser	Connection of strong and weak systems with SCR \geq 1	Independent of systems strength and network without generation	Independent of systems strength and network without generation	Independent of systems strength and network without generation
AC fault ride-through capability	Possible with high risk of commutation failure	Possible with reduced risk of commutation failure	excellent	Very good, but its ability to cope with asymmetrical faults depends on capacitor voltage balancing strategy used	excellent
DC fault ride-through capability	Possible with inherent inductance in the DC side	Possible with inherent inductance in the DC side	Possible with increasing the interfacing reactor $X_L > 0.25\text{pu}$ and current higher rated diodes	Possible with increasing the interfacing reactor $X_L > 0.25\text{pu}$ and current higher rated diodes	Possible with combinations of inherent inductances within each arm and interfacing reactors $X_L > 0.25\text{pu}$ or bypass thyristors
Multi-terminal configuration	limited to 3 due to increase complexity of the control system to achieve current balancing and power reversal	limited to 3 due to increase complexity of the control system to achieve current balancing and power reversal	extendable to any number of terminals practically feasible. DC side isolation is difficult.	extendable to any number of terminals practically feasible. DC side isolation is difficult.	extendable to any number of terminals practically feasible. With single protection zone.
Delivery time	36 month	36 month	24 month	24 month	Not yet known
Redundancy	yes	yes	yes	yes	yes
Manufacturers	ABB, SIEMENS and AREVA	ABB	ABB	ABB	SIEMENS

The cell capacitors are used as energy storage tanks to construct fundamental voltage from predefined discrete steps, and must be sized to handle the fundamental and the 2nd harmonic currents in the converter arm, with minimum cell capacitor voltage ripple. There are several approaches for sizing of the M²C cell capacitance, but can be based on the concept of inertia. The inertia H is defined as the ratio of the electrostatic energy stored in all converter cells to the converter nominal apparent power rating, S_{nom} .

$$H = 6 \times N_c \times \frac{\frac{1}{2} C \left[\frac{V_{dc}}{N_c} \right]^2}{S_{nom}} = 3 \frac{C V_{dc}^2}{N_c S_{nom}} \quad (23.35)$$

$$C = \frac{N_c S_{nom} H}{3 V_{dc}^2} \quad (23.36)$$

For real power transfer, as with HVDC, an inertia H between 30ms to 40ms provides satisfactory performance. N_c is the number of cells per arm, C is the capacitance per cell, and V_{dc} is the pole-to-pole dc link voltage.

Table 23.2 provides a comparison between high-voltage dc transmission system technologies. The comparison focuses on issues such as: control flexibility, fault ride-through capability, conversion losses, electromagnetic compatibility (EMC) issues, and provision of auxiliary functionality such as voltage, frequency, and damping support. The table does not highlight that the MMC converter is most suited to high modulation index, near fixed frequency operation. It cannot function if producing dc output currents, as with ac machine control operating around zero speed (see chapters 10.6.5 and 13.3.4).

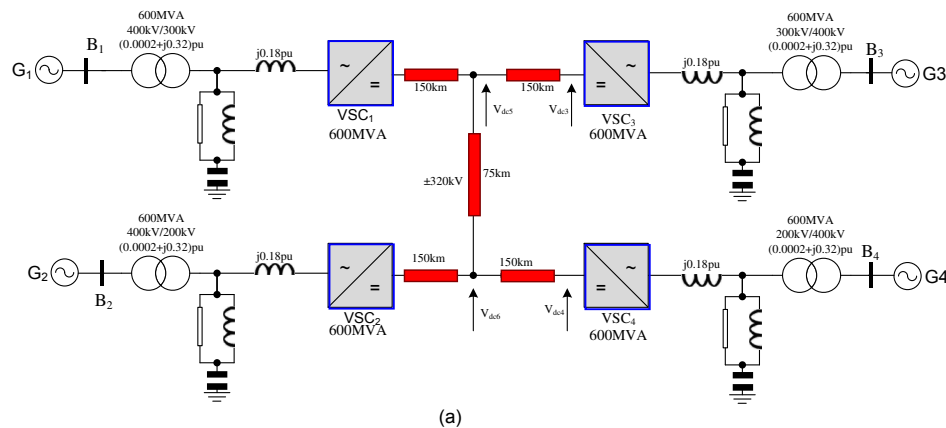
23.12 Multi-terminal VSC HVDC

Multi-terminal HVDC, as shown in figure 23.34, uses VSC topologies where power flow control is achieved with bidirectional converter currents. Figure 23.34a shows a four terminal, mono-polar HVDC topology, while figure 23.34b shows a four terminal, bipolar link HVDC system with the 20 necessary dc breakers/isolators shown as the crossed square symbols.

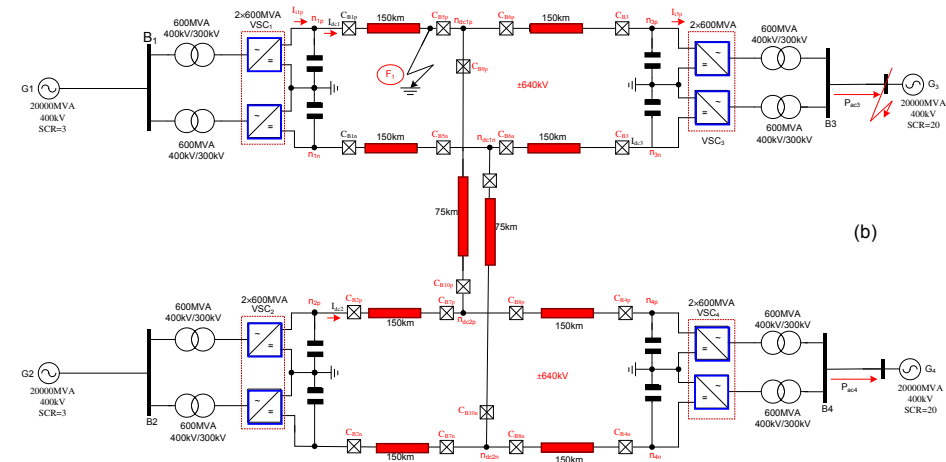
Exploitation of multi-terminal VSC HVDC is hampered by dc fault protection limitations. Even with high transformer leakage inductance of 0.3pu, typical ac currents feeding a dc fault exceed 10pu in less than 5ms, which are experience by the converter freewheel diodes. A purely semiconductor dc circuit breaker can isolated the fault within tens of microseconds, limiting inrush currents to safe levels, but losses are high since the semiconductors are rated for continuous full load current. A hybrid approach of an electromechanical circuit breaker (plus a series IGBT) in parallel with a semiconductor string, is not viable, since electromechanical breaker operation requires a few millisecond, during which time the shunting semiconductors (IGBTs) will unrealistically have to conduct, then commutate, 5 to 10 times rated current.

The alternative is to combine the converter and dc circuit breaker functions by using a converter with dc block capability, as with cascaded H-bridge topologies, at the expense of increased losses.

At a converter, the need for dc circuit breakers is avoided by using the ac side breakers, in conjunction with over-current rated converter diodes and a dc isolator/disconnector. Isolating the other side of the dc side fault is problematic if the remaining parts of the multi-terminal system are to continue functioning.



(a)



(b)

Figure 23.34. Four-terminal VSC-HVDC networks: (a) mono-polar link and (b) bipolar link.

23.13 HVDC Earth Electrodes

Earth electrodes are essential component in a monopolar HVDC transmission system, since they carry continuous operating current. Earth electrodes provide a significantly cheaper solution than a scheme using a second conductor (with half the nominal voltage).

Earth electrodes are also used in all bipolar HVDC systems and in HVDC multi-point systems. All high voltage systems, including HVDC schemes require a reference for voltage measurement, insulation coordination, and overvoltage protection. In a bipolar HVDC system, the station neutral point can be connected to the ground mat of the HVDC station to which the line-side star points of the converter transformers are also connected. Since the direct currents in the two HVDC poles never exactly cancel, in spite of current balancing control, a differential current flows continuously from the station neutral point to ground. It is common practice to locate the grounding of the station neutral point at some distance (10km to 50km) from the HVDC station by means of special earth electrodes.

Earth electrodes for HVDC systems may be land, coastal or submarine electrodes. In monopolar HVDC systems, which exist almost exclusively in the form of sub marine cable transmission systems, there are fundamental differences between the design of anode and cathode electrodes.

i. The Horizontal Land Electrode

If a sufficiently large area of flat land with relatively homogeneous ground characteristics is available, the horizontal ground electrode is the most economical form of a land electrode. The electrode conductor, which is generally of iron, is laid horizontally at a 2m depth, embedded in coke filled trench of 0.5 x 0.5m² cross section. The advantage of this design is in anodic operation, where the passage of the current from the electrode conductor into the coke bed is carried primarily by electrons, and is thus not associated with loss of the material (ions).

ii. Vertical Land Electrode

For high specific resistance surface layers, a vertical deep hole electrode may be viable.

iii. Cathodic Submarine Electrodes

Cathodic submarine electrodes of a monopolar HVDC system with submarine power transmission cable do not present problems. Since there is no material corrosion, a copper cable laid on the bottom suffices, but the cable length should ensure that the surface current density produces an electrical field of less than 3V/m in the surrounding water.

iv. Anodic Submarine Electrodes

Prefabricated electrode modules are lowered to the ocean floor and then connected to the feed cable. When the submarine electrodes are divided into sections which are connected to the HVDC station by means of separate feed cables, the electrode can be remotely monitored.

v. Anodic Coastal Electrode

The coastal electrode is similar in design to the vertical land electrode. Graphite rods surrounded by a coke bed are installed in boreholes which are sunk along the coastline. Such coastal electrodes are readily accessible for inspection, maintenance and regeneration.

A coastal electrode can also be a horizontal land electrode if the ground has the necessary conductivity or if low conductivity can be achieved by irrigating the trench with salt water. With salt water, current flow to the opposite electrode occurs through the water.

23.14 HVDC VSC features

IGBT based systems used in transmission are based around the self-commutating voltage source inverter (VSI) principle; high frequency switching allows converter synthesised controlled voltage at its output. This voltage appears as a power frequency fundamental with harmonics at the switching frequency. With appropriate control, the voltage source inverter may appear as a controlled current source.

The attributes of HVDC voltage source converters allow for simpler ac system integration, plus the following system technological features.

- Independent, continuous control of active and reactive power at each terminal, that is, four-quadrant operational control, down to low power levels.
- Power flow can be reversed instantaneously (50-100ms) without the need to reverse the dc link voltage polarity (only dc current direction reverses), so XLPE (or polarised) cables can be used.
- Steady-state reactive power capability offers voltage control for weak ac grids.
- Independent control of reactive power at each terminal while maintaining full dc voltage for efficient transmission operation. The converter station can be used to provide voltage support to the ac network while transmitting any level of active power, at no additional cost. VSC-HVDC can be configured to provide fast frequency or damping support to the ac networks through active power modulation
- If there is no need to transmit active power, VSC-HVDC can operate in a sleep mode (zero active power exchange) and both converter stations operate as two independent STATCOMs to regulate ac network voltages.
- Dynamic reactive power reserve capability from the voltage source converters for contingency voltage support of the interconnected ac system. The VSC can be connected to blacked-out networks and re-energize them. This feature eliminates the need for a start-up generator in applications where space is critical or expensive such as with offshore wind farms.
- Less filtering requirements, about 15 to 20% of rated power, due to minimal injection of low frequency harmonics, due to PWM modulation. This results in a reduced system installation size.
- No requirement for switched filters or shunt capacitor banks for reactive power compensation with changes in power transfer.
- No inherent fault current contribution to increase circuit breaker interrupting duty. Fault current contribution is naturally limited to maximum load current but can be reduced during faults by fast acting VSC control.
- Robust with respect to ac network faults, thereby allowing continuity of power transmission and limitation of spread of system disturbances.
- VSC HVDC is short-circuit proof for line-to-line-to-ground and line-to-line faults on the dc-side. Good response to ac faults. Since the VSC converter actively controls the ac current, the VSC-HVDC contribution to the ac fault current during is limited to rated current or less, and the converter can remain in operation to provide voltage support to the ac networks provided the ac network remains stable.
- Can operate in ac grids with extremely low short-circuit levels or with passive loads. Can operate in an unsymmetrical network (e.g. during ac network faults) and provide unbalance control to compensate asymmetrical loads. The faster converter response allows counteraction of network distortion and transients.
- Facilitate the development of smart grids, especially during transition from the grid mode to an intended/or unintended islanding mode.

Disadvantages

- Improved control is achieved at the expense of increased losses in the power converter. Increased losses are the result of:
 - i. A higher frequency switching leads to increased switching loss.
 - ii. IGBT devices exhibit higher on-state voltage drop than thyristors with similar voltage ratings. For a given application, this leads to increased conduction loss.
- IGBT modules have lower power capability than available thyristor packages, leading to increased power component count. Footprint is larger than that of thyristors.
- IGBT devices have lower current overload capability than thyristor based systems.
- High dv/dt transients may be present at the output. This can cause problems with cable systems and also electromagnetic interference.
- Higher costs than LCC HVDC.
- DC faults are a serious issue since a VSC behaves like an uncontrolled rectifier bridge during a DC fault. Diode overrating is typically required and the fault is cleared by AC circuit breakers. Typical recovery time for dc faults (assuming AC circuit breaker tripping) is around 10s.
- The development of multi-terminal dc and dc grids requires very fast dc circuit breakers.
- IGBT failure in short circuit is possible but it is much more complex than with thyristors, which naturally fail in short circuit due to disc packaging.
- Higher power losses than LCC HVDC
- Lower power ratings than LCC HVDC

The progression and expansion to multi-terminal HVDC systems is hampered by the fact that VSC technology cannot inherently block the ac side from the effects of dc-side faults.

23.15 HVDC LCC features

The main advantages of LCC HVDC include:

- Thyristor devices have low losses and are available in robust high voltage (6-10kV), high current (3-4kA) capacity single wafer capsules
- Thyristors have excellent overcurrent capability
- Thyristors, in disc packaging, naturally fail in short circuit which is desired for high-voltage valves
- Thyristor costs are lower than IGBT costs
- Line commutated HVDC has an established track record at transmission voltage and power levels.
- Resilience to dc side short circuit faults. The system can operate well at low dc voltage and dc fault recovery is well controlled.
- Provides ac system frequency stabilisation in most installations, but performance is limited because of reactive power issues. AC voltage control can also be implemented.

The disadvantages of LCC HVDC are:

- Inject significant low order harmonics which must be eliminated using large (physically and electrically) passive filter arrangements. The presence of these filters may lead to circulating harmonic currents which must be mitigated by damping networks. Filters and damping networks may have to be designed specifically for each location and may not be optimum for all operating conditions.
- Inherently limited in their response time (limited to line frequency switching) and may face limits to their control ability. For example thyristor based HVDC:
 - Cannot decouple the real and reactive power injected into the network.
 - Requires large reactive power compensation. This reactive power is supplied using passive filters and switched capacitors and reactors. The switched banks are required since the amount of reactive power needed varies with the active power magnitude and operating mode (inversion or rectification). As a result, the HVDC converter station based on line commutated converters is bulky and has a large footprint.
- Power reversal necessitates the dc link voltage polarity be reversed. The XLPE cables have a range of cost and performance advantages over traditional paper/oil insulated dc cables, but they can not take fast voltage polarity reversal. Also, the time required to reverse the power flow is limited to around 0.5s, which imposes operational constraints.
- There is a theoretical minimum power flow of 10% in the dc link to guarantee satisfactory operation.
- It is only suitable for connection of the ac networks with a high short circuit ratio (SCR > 2.5).
- Suffers from commutation failure (dc-side short circuit) during ac faults. Typically a sudden ac voltage drop of 5-10% will cause commutation failure. A commutation failure causes transient (0.5-1s) interruption in power transfer.

- Vulnerable to dc side open circuit conditions. This is an unlikely event and causes overvoltage which is readily limited by surge arresters.
- Multi-terminal topologies can be built but with performance and cost penalties. DC grids are challenging.

23.16 Features of conventional HVDC and HVAC transmission

The following are comparison features between ac and conventional dc electrical power transmission:

- Increased power system stability since dc power flow is controlled by converter delay angles. Converter response times are of the order of ms, while the dc link-time constant is significantly longer. Thus, the dc-link short circuit current can be limited.
- No distance effect on stability (voltage angle), with dc transmission, plus no intermediate stations needed every few hundred kilometres.
- The fast converter response times means power reversal can be achieved in ms, much faster than within ac systems.
- Steady-state power flow is related to dc-link resistance, as opposed to ac-line reactance.
- Transmission line inductance has zero impedance to dc, whereas inductive reactance is relatively large in ac systems. A minimal ac skin effect occurs with ac transmission.
- AC power is lost due to dielectric losses. Capacitance between conductors is open circuit to dc, but in ac systems capacitive reactance current paths exist which increase I^2R losses.
- Under sea cables have high capacitance which has minimal effect on dc transmission
- DC back-to-back converters (with minimal link inductance, tens of millihenry's) allow synchronisation between 50Hz and 60Hz systems or same frequency systems at different voltage phase angles.
- DC transmission line and its towers are cheaper per unit length than for ac, but dc terminating stations are more complicated and expensive than ac terminating stations
- DC converters have limited overload capability and are less reliable because of the ancillaries (filters, cooling management, etc.).
- DC transmission can have a lower visual impact, plus a narrower corridor, hence lower environmental impact than ac systems
- Electric and magnetic fields for dc transmission have lower environmental implication than ac fields
- Corona effects tend to be less significant with dc than for ac conductors
- DC transmission is more robust to lightning effects, since more effective surge protection is used.
- Polymer cables age slower, giving a longer lifetime, with dc
- Maximum voltage gives lower I^2R losses for a given transmitted power level
- No unnecessary energy transfer since no reactive VAR ($S=VI^*=P+jQ$), with dc

The general advantages of ac transmission, over dc transmission, are

- No costs associated with ac-dc-ac conversion equipment
- Transformer (and autotransformer) voltage matching
- Reactive power and harmonics readily compensated
- Not restricted to only point-to-point connection, as is HVDC (there is no fully functioning exception)
- Established system control methods
- No ac transformer dc voltage stressing due to asymmetrical phase control alignment, and no I^2R and core losses due to high harmonic currents
- ac switch gear and breakers, (and particularly vacuum circuit breakers up to 33kV) are very effective - compared with the difficulties in breaking dc current
- Lower current harmonics

Reading list

Mohan, N., *Power Electronics*, 3rd Edition, Wiley International, 2003.

Acha, E., *et al.*, *Power Electronic Control in Electrical Systems*, Newnes, 2002.

HVDC Connecting to the future, Alstom Grid, 2010

Problems

23.1 Show that if a three-phase ac transmission system is converted to a tripole hvdc system with the third conductor transmitting a square-wave current of ± 1 pu, that the other two phases can alternately conduct $\frac{1}{2}(\sqrt{3}+1)$ and $\frac{1}{2}(\sqrt{3}-1)$, yet not exceed their thermal rating.

23.17 Appendix: HVDC topology classification

Figure 23.35a shows the symmetrical mono-polar HVDC link configuration, which has the following advantages and disadvantages:

- Since the virtual supply mid-point is established by dc cable stray capacitances, the converter transformers are not exposed to dc voltage stresses;
- no ground dc current;
- no ac current contribution from the grid during a pole-to-ground dc side fault; and
- requires two fully insulated dc cables and no redundancy; so tends to be an expensive solution.

Figure 23.35b shows an asymmetrical mono-polar VSC-HVDC link with a metallic return. The main advantages and disadvantages of this configuration are:

- Metallic ground cable is not fully insulated, hence reduced expenditure on the dc cables;
- no dc ground current;
- permits extension to a bi-polar configuration;
- exposes the interfacing transformer to dc voltage stresses; and
- no redundancy.

Figure 23.35c shows asymmetrical mono-polar VSC-HVDC link with ground return, where the main features and drawbacks of this approach are:

- Uses a single dc cable, which reduces cost and transmission losses;
- allows extension to a bi-polar link;
- no redundancy;
- exposes transformer to dc voltage stresses;
- with ac current in-feed from the ac side, a pole-to-ground fault exposes the converter switches to increased current stresses; and
- causes environmental concerns due to the use of grounded electrode and continuous operation with ground current, hence requires special permit.

Figure 23.35d shows symmetrical bipolar VSC-HVDC link with ground return. The main benefits and shortcomings are:

- Does not expose converter transformer to dc stresses;
- no ac current in-feed from the grid during pole-to-ground dc network faults;
- dc link capacitors and cable insulation must be rated for the full dc voltage; and
- requires permission to operate with ground return during outage of one dc cable (ac current in-feed exist).

Figure 23.35e shows a symmetrical bi-polar VSC-HVDC topology with metallic return. This configuration has the following advantages and disadvantages:

- 50% redundancy of total rating;
- suffers from ac current in-feed from the grid during a pole-to-ground dc fault;
- transformer must be designed withstand dc voltage stresses; and
- use of electrodes causes environmental concerns, therefore requires permission.

Figure 23.35f is a symmetrical bi-polar HVDC link with metallic return with the following features:

- 50% redundancy of total rating;
- no ground current;
- increases transmission capacity, without the need to raise converter dc link voltage; and
- exposes transformer to dc voltage stress.

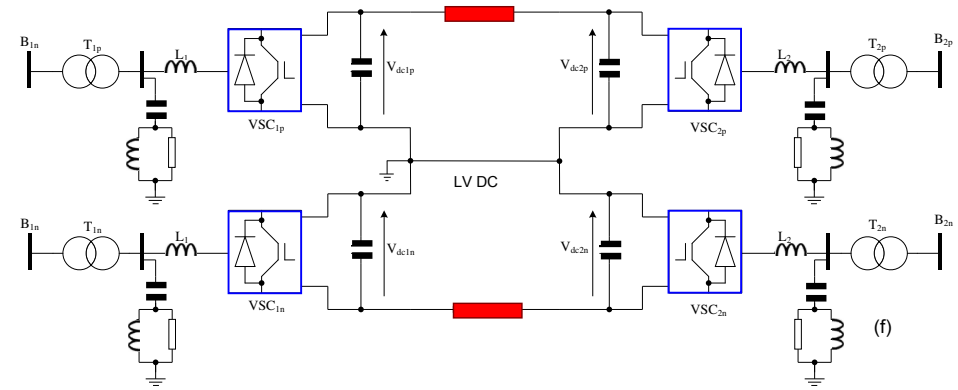
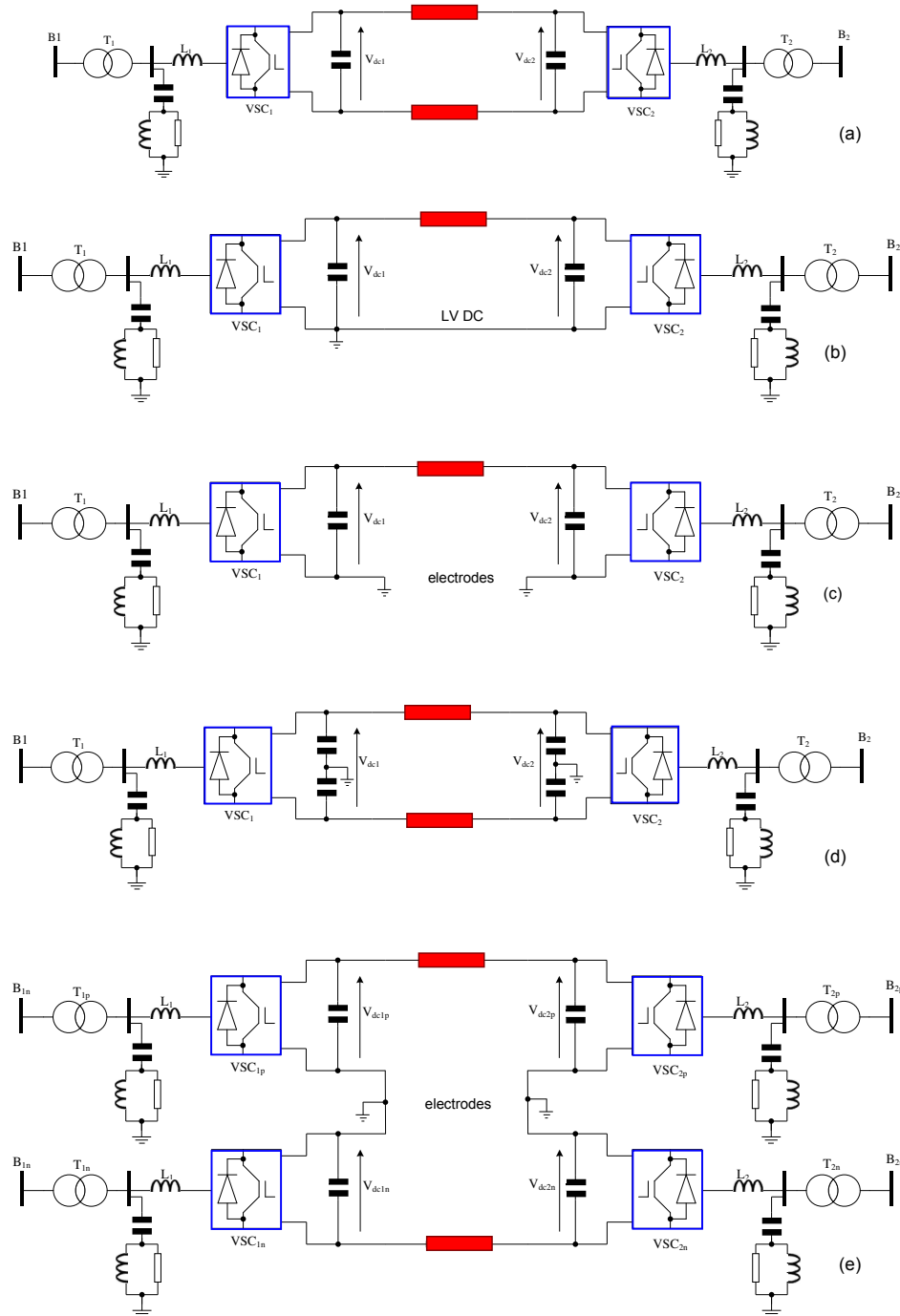


Figure 23.35. Different mono-polar and bipolar VSC-HVDC topologies: (a) symmetrical mono-polar link, (b) asymmetrical mono-polar link with metallic return, (c) asymmetrical mono-polar link with ground return, (d) symmetrical bipolar link with floating ground return, (e) symmetrical bipolar link with ground return, and (f) symmetrical bipolar link with metallic return.